Chapter 7
Active Sites for Selective Catalytic Reduction

Wolfgang Grünert

7.1 Introduction

The "active site" is a central concept in catalyst research introduced by H. S. Taylor in 1925 [1]. It describes an ensemble of atoms in a solid surface which takes part in the rate-limiting step of a catalytic reaction mechanism. This is the stage on which the catalytic reaction spectacle plays, traditionally as thought without yet the actors. The practical importance of knowing the active site is obvious: once its structure is determined one can search for routes to prepare it in larger abundance for making better catalysts. It is important to note that solid surfaces are dynamic and respond to the properties of the reaction medium. Therefore, the actual active sites are often formed from precursor structures only under reaction conditions, and there are even cases where they disappear when these conditions are changed beyond certain limits (e.g., carbided Pd surface layers for selective hydrogenation of dienes [2]). Still, the active site concept describes only the solid-state aspect of the full picture, but the example shows that active sites can be reliably identified only under real reaction conditions.

This adds yet another aspect of complexity to a task which is challenging in itself: the search for the active sites. Catalysis occurs on metastable structures rather than on idealized stable surfaces, which usually offer low activities (=reaction rates related to surface area under specified conditions as temperature and reactant composition). We have to look for defect sites, for atomic arrangements to be found only on small particles, on interaction structures with a second component, e.g., a support or a promoter. Usually, the arrangement of atoms requested by the catalytic reaction is not the only one exposed by the catalytic element. The coexistence of the active sites with indifferent structures or even with sites catalyzing the same reaction with different activation energy and, therefore

W. Grünert (✉)
Laboratory of Industrial Chemistry, Ruhr University Bochum, D-44801 Bochum, Germany
e-mail: w.gruenert@techem.rub.de

I. Nova and E. Tronconi (eds.), *Urea-SCR Technology for deNOx After Treatment of Diesel Exhausts*, Fundamental and Applied Catalysis,
DOI: 10.1007/978-1-4899-8071-7_7,

capable of dominating the catalytic behavior in a different temperature range, offers a considerable methodical challenge to any research effort.

Obviously, the search for the active sites of a reaction is a very involved task requiring the concerted application of various techniques to well-selected catalytic materials, desirably under reaction conditions. Even then progress toward reliable identification of the responsible structures may be slow due to the complexity of the catalytic surfaces. There is, however, an additional rationale for such research, because the data generated are often of considerable value for practical catalyst development. Therefore, the literature is full of opinions about active sites on catalysts for various reactions, which may be everything from well-supported proposals down to mere speculation.

The present report gives a critical overview on the state of knowledge about active sites for SCR of NO by ammonia over the most important catalysts known today. As indicated in earlier chapters, this actually involves two reactions—standard SCR (reduction of NO by NH_3 in presence of O_2, Eq. (7.1)) and fast SCR (reduction of equimolar NO/NO_2 mixtures by NH_3, in presence or absence of O_2, Eq. (7.2)). Due to recent discussions on reaction mechanisms (see Chaps. 8 and 9), the oxidation of NO to NO_2 (Eq. 7.3) will be briefly considered as well.

$$4NO + 4NH_3 + O_2 \rightarrow 4N_2 + 6H_2O \tag{7.1}$$

$$2NO + 2NO_2 + 4NH_3 \rightarrow 4N_2 + 6H_2O \tag{7.2}$$

$$2NO + O_2 \rightarrow 2NO_2 \tag{7.3}$$

Initially, a short overview over the methodology used in pertinent studies will be given. The subsequent discussion will focus on the traditional V_2O_5–WO_3/TiO_2 system and on zeolites modified with transition-metal ions ("TMI") as Fe and Cu, and only briefly touch upon new catalyst systems on the basis of Mn or Ce. The questions to be answered concern mainly the structure of the redox sites: Are they isolated TMI sharing oxygen bridges only with the support, or are they surface bound oligomers, islands, three-dimensional clusters? How does the promoter operate? Is there an influence of cation exchange positions in zeolites on activity? Is there a primary role of acidity, e.g., Brønsted sites being part of the active site, or does acidity just increase local NH_3 concentrations?

7.2 Strategies and Methods for the Identification of Active Sites

Active sites can be identified if there is a correlation between the abundance of the corresponding structural motif in a catalyst type (desirably detected under reaction conditions) and the catalytic activity. To identify such relations, one has to apply suitable methods for the structural analysis of disordered material (geometrical and

electronic structure) to either a series of catalysts which offers the whole variety of candidate species in sufficiently different concentrations, or to one catalyst on which this variety can be produced by chemical manipulations (e.g., sinter series). The resulting structural data have to be correlated to meaningful reaction rate data from all these materials. Therefore, the most popular structure characterization techniques will be reviewed in the following with respect to their potential for this kind of study. For the basics of these methods, the reader is referred to the pertinent introductory and advanced literature [3–7]. In such studies, situations may be encountered where two or more different species types are obtained in similar ratios in all preparations applied and therefore cannot be discriminated with respect to their catalytic relevance. Transient approaches suitable for such situation will be briefly outlined as well.

Although an ever growing choice of spectroscopic, diffraction, imaging, and sorption techniques are available to the catalytic scientist, none of them is really well adapted to the problem to be solved here. Therefore, studies on active sites generally employ a multitude of methods. Catalysis is a surface phenomenon, but hardly any technique is ideally surface sensitive—with the exception of adsorption methods, IR spectroscopy if performed on interacting probe molecules, and Ion Scattering Spectroscopy[1] (ISS). However, methods probing near surface regions or even the bulk of the material may be still of great value for the identification of active sites when the signals detected are dominated by information from the surface due to a high or even atomic dispersion of the phases under study. This tends, however, to exclude diffraction techniques, in particular XRD, because coherence lengths available from such disperse phases will fall short of those required for achieving detectable diffraction signals.

Despite impressive progress in resolution and contrast utilization, *imaging methods* like electron microscopy or scanning probe microscopy play only a supporting role in active site studies. Although atomic details of real surfaces can now be made visible, the quantification of sites for correlation with activity and the statistical significance of the small assay remain problematic. Imaging, however, can be extremely helpful for the interpretation of data from statistically more representative though more indirect techniques. Examples are the visualization of morphological changes in Cu particles interacting with ZnO at different redox potentials [8], which had been predicted on the basis of EXAFS data [9, 10], and the detection of surface amorphization of a mixed Mo–V–Te–Nb phase during selective propane oxidation [11, 12], which had been previously observed by XPS (in situ [12] and under vacuum [11, 13, 14]) just as deviations between surface and bulk compositions.

X-Ray absorption fine structure (XAFS) is a powerful technique for the study of active sites, but certain limitations have to be taken into account. It is an averaging method: information arising from all kinds of species formed by the element of

[1] Alternative designation—Low-energy Ion Scattering (LEIS).

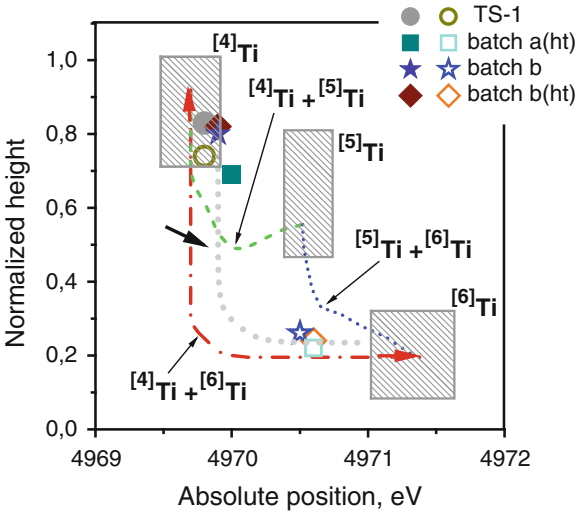

Fig. 7.1 Analysis of Ti coordination geometry by Ti*K* pre-edge signal position and intensity [15], applied to a mesoporous material with expected TS-1 wall structure. Ti in three batches is tetrahedrally coordinated in dehydrated state (*full symbols*), but almost completely sixfold in hydrated state (*open symbols*), expect for the hydrophobic crystalline TS-1. Reproduced from [19] with permission of Elsevier

interest is superimposed. If the spectra of the candidate species are known, this superposition can in principle be used for a quantitative analysis of species concentrations. This is often done for the *N*ear-*E*dge region (XANES) which reflects only the first coordination sphere, but it is much more complicated for the *E*xtended *X*-Ray absorption fine structure (EXAFS) which usually probes structure to larger distances. It has been sometimes disregarded that coordination numbers extracted from EXAFS fits must not be used to construct the typical coordination sphere of an element if the latter has formed more than one species type. In such situation, which can be sometimes but not always diagnosed from the XANES, EXAFS can still provide valuable information, which is however less reliable and quantitative. The potential of the XANES to give access to the distribution of oxidation states or coordination geometries (pre-edge signals of first-row TM ions, e.g., Ti [15], V [16], Fe [17, 18]) is often used to characterize the state of an element in in situ or *operando* studies during catalytic reactions. Figure 7.1 shows an example dealing with ordered mesoporous materials the walls of which were claimed to consist of titania silicate TS-1 nanoslabs [19]. Position and intensity of the pre-edge peak confirmed the tetrahedral coordination of the Ti while the decay and shift of this signal upon hydration (unlike with the hydrophobic crystalline TS-1 reference) proved its accessibility.

The recent development of wavelength differentiating fluorescence detection (HERFD—high energy resolution fluorescence detection) together with the increased brilliance of synchrotron sources has initiated large progress in the differentiation of coexisting species by X-Ray absorption methods (reviewed in [20]). Detection of spectra using fluorescence lines with small lifetime broadening (K_β) instead of intensity in a broad energy range permits more detail to be seen in the chemical sensitive pre-edge features. If there are sufficient differences between the K_β fluorescence signals of species involved, EXAFS spectra predominantly

reflecting the coordination sphere of one or the other site can be acquired by appropriate setting of the detector. The measurement of fluorescence spectra tuning the excitation energy through the energy range of a XANES (RIXS—Resonant Inelastic X-Ray Scattering) creates a two-dimensional array offering rich structural information. The broader introduction of these techniques into catalyst research bears great promise for the structural analysis of real systems.

Another interesting version of XAS suitable for active site studies is soft X-Ray absorption spectroscopy. The L edges of first-row transition metals often bear a considerable diagnostic potential for the identification of oxidation states and coordinations, which at present is largely disregarded in catalysis research.

X-Ray photoelectron spectroscopy (XPS) is well known as a method for quantitative determination of surface compositions, including the differentiation of oxidation states of elements. While being primarily an elemental analysis, its potential to diagnose coordination geometries is weak although such conclusions may be sometimes indirectly drawn from the identification of surface compounds. Such analysis is often possible by combining binding energies of XPS lines with the kinetic energies of X-Ray-induced Auger lines that appear as a by-product of the photoemission process (Auger parameter). The information provided by conventional XPS may be highly relevant for active site studies although it does not characterize the external surface layer but averages over a near-surface region of a few nanometer thickness. The ultra-high vacuum requirement of the method, however, is a clear disadvantage. The advent of an in-situ version of XPS (APPES—ambient pressure photoelectron spectroscopy), where spectra can be measured under some millibar pressure at the sample, was therefore a breakthrough [21]. It has been made possible by combining differential pumping stages, which had been long known, with electron lenses [22] as indicated in Fig. 7.2.

Regarding vibrational methods, the potential of *Raman spectroscopy* to analyze surface oxide phases has been widely applied to supported oxide catalysts [23], in particular with Raman-inactive supports. Resonance Raman spectroscopy, which involves excitation of Raman spectra at wavelengths where species present exhibit an absorption maximum, offers additional opportunities for structural characterization. *IR spectroscopy* where the region of lattice vibrations used for such purpose is too complex to be productive, is highly useful for the detection of adsorbates and reaction intermediates. However, the characterization of surface structures by IR spectroscopy of probe molecules, e.g., of acidic sites by adsorbed N bases, has been a long tradition as well. Probe molecules can trace the degree of coordinative unsaturation of surface species as demonstrated, e.g., in classical studies of the Zecchina group on the characterization of supported Cr oxide species ([24] and subsequent series of publications). Their ability to discriminate between cationic adsorption sites allowed creating the experimental basis for the CoMoS model of promoter interaction in hydrodesulfurization catalysts [25]. The potential of CO to differentiate between different oxidation states of an element [26, 27] has been often applied as well. In reactions involving CO, it has been used to directly probe the exposure of different species to the reaction atmosphere, including the response of the active site distribution to changes of reaction conditions [27].

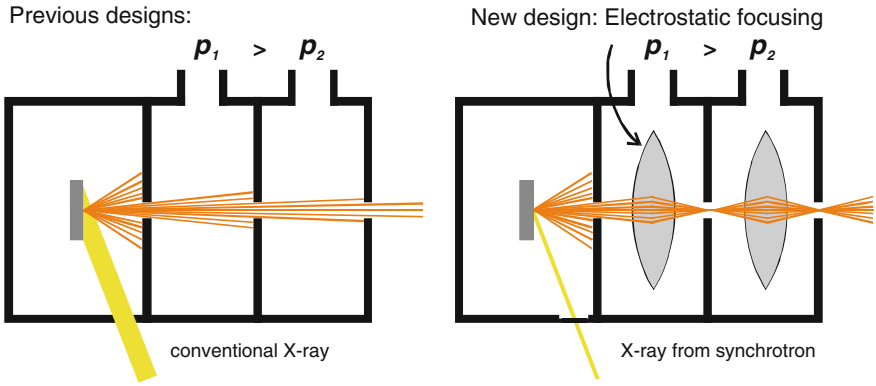

Fig. 7.2 Ambient pressure photoelectron spectroscopy: combination of differential pumping with electron optics to allow for realistic photoelectron yield from in situ cells. Reproduced from [21] with permission from Elsevier

Absolute concentrations are, however, often difficult to establish due to the lack of information on extinction coefficients and due to different adsorption probabilities under the prevailing conditions. Instructive examples for research along these lines are the observation of Cu–Zn interactions in working methanol synthesis catalysts [28] and of coexistence of metal and ionic Ru sites in alumina-supported Ru catalysts for partial oxidation of methane [29].

UV–Vis spectroscopy is another technique often used in active site studies. In the visible region, the d–d transitions are related to valence states and coordination geometries (ligand field symmetries) of cations, at shorter wavelengths ligand-to-metal charge-transfer transitions between filled orbitals with mainly ligand character and empty cation states appear, which are sensitive to the aggregation degree of the corresponding phase. While UV–Vis spectroscopy is popular as an in situ technique and yields to quantification more readily than IR spectroscopy, its limitations are related to the considerable width of the signals and to problems with line superposition and interpretation (cf. "Fe Zeolites" section).

EPR spectroscopy detects species with magnetic moments arising from electron spins, often with extraordinary sensitivity. Among them, signals from systems with an even number of unpaired spins can be obtained only at very low temperatures due to short relaxation times. EPR signals of isolated cations bear information about the symmetry of their ligand field, the identity of the cations can be judged upon by a hyperfine splitting if there is a nuclear momentum, sometimes by the signal position (g values). Disordered aggregates of paramagnetic sites cause interaction broadening of signals down to complete loss of intensity, whereas ordered arrays may lead to exchange narrowing. Collective spin coupling phenomena may be identified by measuring spectra in a wide temperature range. This is exemplified in Fig. 7.3 by comparing the temperature dependence of the EPR spectra of three Fe–ZSM–5 catalysts, where the isotropic signal at $g' = 2$ increases

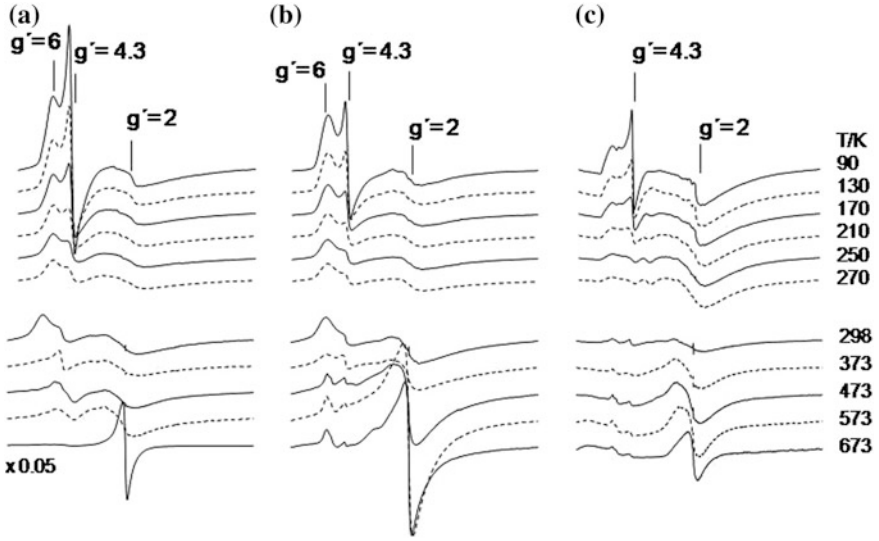

Fig. 7.3 Temperature dependence of EPR spectra of Fe–ZSM–5 catalysts prepared from H–ZSM–5 and $FeCl_3$ via different routes. **a** Solid-state ion exchange, **b** Chemical vapor deposition, **c** Mechanochemical treatment. The intensity variation of the signal at $g' = 2$ measured above the Neel temperature (e.g., at 673 K) indicates the clustering degree of the Fe-oxide phase. Reproduced from [30] with permission of Elsevier

to different extents at high temperatures indicating different clustering degrees of the Fe-oxide aggregates present [30].

EPR intensities are proportional to spin concentrations as long as the spins are not interacting very intensely. Quantitative analysis requires double integration of the signals and the availability of reliable spin standards. It is prone to uncertainties and therefore rarely performed. EPR is often used to characterize systems composed of d^0 ions by measuring the signals of d^1 defects which occur in the d^0 phases for entropy reasons. While this is a very useful approach, one should be cautious with quantitative conclusions because the percentage of defects is unknown and may vary among the phases present. EPR can be also performed in situ and even *operando*, provided the heating of the sample can be made without interference with the microwave field required for the measurements. The technique is described in [31].

Similar to EPR, solid-state *NMR spectroscopy* has a limited range of applications, which is defined by the magnetic moment of the corresponding elemental nuclei. While EPR may detect extremely low concentration of paramagnetic sites, NMR has sometimes sensitivity problems, in particular in the case of nuclei with low natural abundance, e.g., ^{13}C or ^{15}N. There are, however, various techniques for signal enhancement, the best known being cross-polarization where magnetization is transferred from an abundant to a dilute spin site. Information on coordination geometries, which is encoded in the g tensor in EPR, is eliminated in solid-state

NMR by the magic angle spinning technique: the NMR parameters achieved are scalars. NMR signals are greatly perturbed if there is an unpaired electron at the atom of interest.

Nevertheless, solid-state NMR can be useful for active site studies, which is nowadays predominantly employed for acid catalysis, e.g., with zeolites [32]. Chemical shifts obtained are related to the electronic state of the atom: ^{1}H–NMR data have been, for instance, used to determine acidity of Brønsted sites in zeolites, ^{51}V NMR can discriminate V^{5+} in various environments in supported catalysts [33]. As long as the sites are sufficiently dilute, NMR intensity is directly related to concentration. Structural information is accessible by echo techniques which allow determining distances between spin sites. By analogy with IR methodology, adsorption sites have been investigated with probe molecules also in NMR studies. While work with N bases may require isotopic enrichment of the probe, there are opportunities to detect subtle structural features by cross-polarization and double-resonance (e.g., ^{14}N/^{27}Al) techniques [34].

The in-situ application of solid-state NMR requires heating and temperature control of the spinning sample. Techniques available for this purpose are reviewed in [35]. The method is applied preferentially for mechanistic rather than for active site studies, but the former often result in indirect conclusions on the sites involved in the detected reaction mechanisms [32].

Moessbauer spectroscopy is readily applicable only for a few elements that exhibit suitable low-energy nuclear transitions on which the method is based—to Fe, Sb, and Sn. For measurements with Ru, Ir, Pt, and Au, one faces a number of complications (low measurement temperatures, dependence on sources with short half-lives, working at synchrotrons, etc.). Co is accessible by inverse Moessbauer spectroscopy, which requires preparation of the sample with ^{57}Co, the isotope that decays into the source nucleus ^{57}Fe.

Such effort can be justified due to the high diagnostic potential of the method for structural features. The spectra indicate the electronic state of the element (including high-spin/low-spin differentiation), asymmetries in the coordination sphere, and the intensity of magnetic interactions between the atoms. In the case of iron, size determination is possible for superparamagnetic clusters. Due to the temperature dependence of the recoil-free fraction that determines the signal intensity from the corresponding structure, the spectra from samples containing iron in states of different dispersion may change with temperature, and also under the influence of an external magnetic field, which gives the chance to single out contributions from different coexisting sites.

Figure 7.4 shows an example where Moessbauer spectroscopy revealed the presence of Fe-oxide aggregates in Fe–ZSM–5 prepared by chemical vapor deposition of Fe according to [36], which was expected to contain the Fe species in nearly atomic dispersion from the EXAFS spectra [37]. This was based on the very low intensities of Fe–Fe scattering between 2 and 3 Å, uncorrected, which can be seen in Fig. 7.4a, and the lack of significant scattering intensity above 4 Å, which suggests nearly ideal dispersion of Fe. At the same time, sextets in the Moessbauer spectra in Fig. 7.4b, c clearly show the presence of large oxide aggregates. The

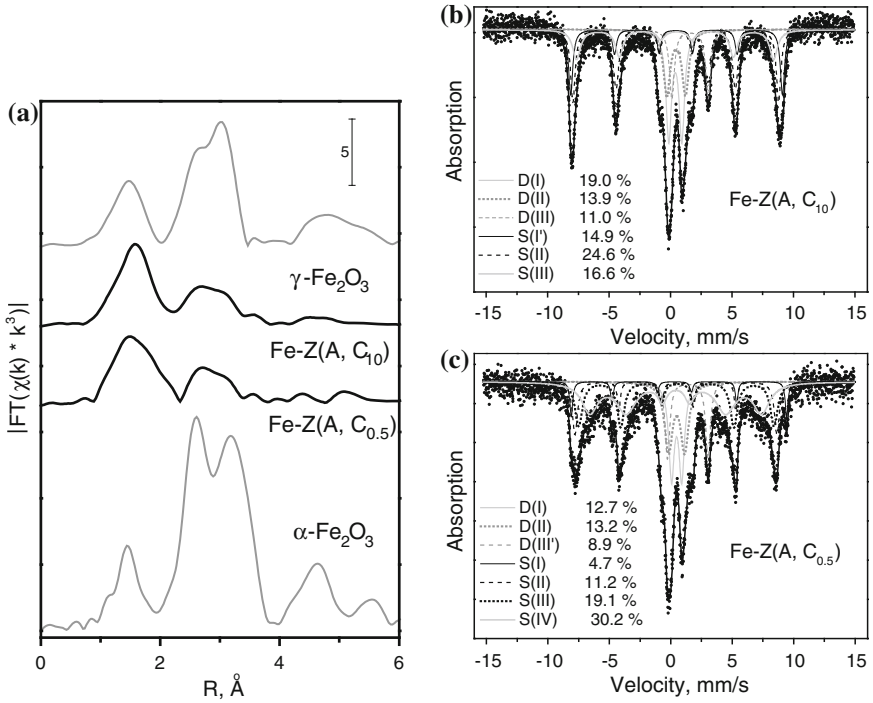

Fig. 7.4 Fe-*K* EXAFS (**a**) and Moessbauer spectra (**b**, **c**) of two Fe–ZSM–5 catalysts prepared by CVD of $FeCl_3$ into H–ZSM–5 and calcined with different heating protocols. The missing order at higher distances in the EXAFS spectra suggests the absence of larger aggregates, which are, however, clearly indicated by the Moessbauer spectra. Reproduced from [37] with permission of Elsevier

contradiction apparently resulted from large disorder in the particles, which may have included debris from destroyed zeolite structure. Such disorder would prevent the observation of EXAFS scattering paths and cause anomalies in the Moessbauer parameters as obtained in the fits to Fig. 7.4b, c [38].

There have been so far no in situ Moessbauer studies with catalysts, most likely due to the loss of intensity (recoil-free fraction) and of particle size differentiation with increasing temperature.

The methods discussed so far are particularly qualified for active site studies by offering the potential for in situ work—even in electron microscopy, an "environmental" version in which the sample is kept under some millibar of reactant pressure is available nowadays. Valuable insight into the structure of surfaces can be, however, also obtained by methods targeting adsorptive interactions of reactants or other probe molecules with the surface although these are usually performed in separate experiments, e.g., on catalysts previously subjected to reaction conditions.

Volumetric *chemisorption* techniques are widely used to explore the particle sizes (actually the size of the accessible surface) of dispersed metals. With oxides and sulfides, they measure the total coordinative unsaturation of the surfaces, which may be related to the catalytic properties. The energetic effects of adsorption are probed by *adsorption microcalorimetry*, which gives frequency distributions for sites with different interaction strength with the adsorbate, without of course providing information about the structural features of the detected sites. Adsorption interactions are often probed by reverting the process. For instance, desorption into a carrier gas under a (linear) temperature increase (*temperature-programmed desorption, TPD*) gives the chance to differentiate the sites according to their interaction strength with the adsorbate, though with less accuracy than calorimetry. Even nearer to catalysis is *temperature-programmed surface reaction (TPSR)*, where an adsorbate is reacted under a linear temperature profile with a reactant offered in a carrier gas. This can reveal the existence of different active sites for a reaction and give access to energetic properties of the existing sites.

Temperature-programmed reduction (TPR) and temperature-programmed oxidation (TPO) are thermal methods related to transformations of the catalyst rather than to adsorption on its surface. The former differentiates phases in the catalyst according to their reducibility, the latter, which is usually performed after having had a (redox) catalyst in a steady state with the reactant flow, probes the average reduction degree of the elements present and differentiates components according to their tendency to be reoxidized.

All thermal methods mentioned are highly productive in indicating differences between the catalysts prepared and known phases or in detecting changes by treatments, without giving any hint on the nature of species formed during preparation or further processing. Combinations of such methods with techniques of structural analysis have rarely been described in the literature. There is a special opportunity for TPD, because a version of this method (*TDS—Thermal desorption spectroscopy*) is used in surface science to investigate the adsorption properties of ideal well-characterized surfaces. Indeed, comparison of activation energies of desorption obtained by TPD of H_2 from real Cu catalysts with analogous H_2 TDS data from Cu single crystal surfaces has been used to judge upon the exposure of Cu facets in methanol synthesis catalysts [39].

The characterization techniques discussed so far are summarized in Table 7.1.

The discrimination of the active site among coexisting inactive or less active structures requires a set of samples containing the candidate species in sufficiently different abundances. A situation where such samples are not accessible by the preparation methods employed calls for *transient methods*.

Catalytic mechanisms of redox reactions most frequently involve redox cycling of (a) transition-metal ion(s) contained in the active site. Under reaction conditions, the oxidation state of the TMI in coexisting sites will adapt to the redox potential of the reaction medium in different ways depending on the redox properties of the individual structures. The different oxidation states observed under stationary reaction conditions are, however, not related to the relevance of the corresponding sites in the catalytic process because for the active site, all oxidation

Table 7.1 Characterization techniques used in heterogeneous catalysis and their potential for the identification of active sites

Technique	Potential	Limitations	In situ/ operando?
XRD	Determination of long-range order, of particle sizes	Averaging technique, on traditional level no potential for disordered structures	yes
Electron microscopy	Visualization of structures down to atomic details, usually in UHV, but environmental versions available	Site concentrations difficult to establish, analysis refers to small assay of material under study (support by averaging technique desirable)	in situ (limited)
XAFS (EXAFS/XANES)	Short-range order, also for disordered or highly disperse phases, electronic structure	On traditional level averaging technique, difficult for situations with many species of an element coexisting	yes
XPS	Atomic concentrations, oxidation states in near-surface layer, sometimes structural information, UHV technique, environmental versions available	Averaging over sampling region (depth differentiation requires synchrotron source[a]), assignment of signals may be complicated, structural information limited	in situ (limited)
LEIS (ISS)	Identification of atoms in topmost layer, concentration gradients via sputter series, vacuum technique	No information on oxidation states, averaging technique, concentration analysis possible, but with risks	no
Raman	Structural information for highly disperse phases, characterization of adsorbates	Qualitative, signal superposition for complex materials, problems with sample fluorescence	(yes)
IR	Characterization of sites (acid–base, redox) by probe molecules, of adsorbates, structural information	Concentration analysis difficult (only in transmission geometry, extinction coefficients required), structural information often limited by signal saturation	yes
UV–Vis	Analysis of oxidation states, of aggregation degree of TMI sites	Semiquantitative, broad signals may create problems with assignment, poor resolution of clustering degrees	yes

(continued)

Table 7.1 (continued)

Technique	Potential	Limitations	In situ/ operando?
EPR	Analysis of paramagnetic sites and their environment, extremely sensitive, gives information also on clustered phases	Not all oxidation states accessible, accuracy of concentration analysis limited	yes
NMR	Concentration, coordination, oxidation states of elements, sometimes information on distances between sites	Only nuclei with nonzero spin, sometimes problems with sensitivity, interference by nearby paramagnetic sites complicates application in redox catalysis	yes
Moessbauer	Oxidation states, coordination to neighbors, clustering degrees of sites	Only a few elements with suitable nuclear levels, in particular Fe, full diagnostic potential only at very low measurement temperatures	no[b]
Chemisorption	Particle sizes (metals), adsorption sites (ionic surfaces)	Particle size determination averaging; adsorption stoichiometry not always clear	no
Adsorption calorimetry	Enthalpy and entropy of adsorption (titration method) for probe molecules and reactants	Limited to simple systems (well-defined surface, one adsorptive)	no
Temperature-programmed desorption	Differentiation of adsorption sites on a surface, depending on test molecule for acid/basic or redox sites, determination of energetics of desorption	Desorption signals remain to be assigned to sites	no
Temperature-programmed reduction/ oxidation	Reduction/reoxidation properties of redox phases in samples; strong in detecting interactions between phases, in simple cases determination of energetics of reduction	Nature of detected interactions remains to be elucidated	no

[a] Angle-resolved XPS, which can be performed with lab sources, is a safe tool only for flat sample surfaces

[b] In principle possible, but no examples known; loss of diagnostic potential at elevated temperatures seems to discourage attempts

states are possible: the actual situation is determined by the ratio between reduction and reoxidation rates, slow reoxidation resulting in low stationary oxidation states, and slow reduction in a fully oxidized site. Therefore, reduction and reoxidation rates have to be measured under typical reaction conditions, e.g., as a response to step changes of the feed composition. Sites in which any of the two rates is clearly lower than the stationary reaction rate may be rejected. More challenging but at the same time more promising is to compare how the oxidation states of the TMI in coexisting sites on one hand and the reaction rate on the other respond to step composition changes. Such step change will usually cause a change of both reaction rate and oxidation states of all coexisting sites, but only for the site causing the observed reaction will the transient response of the oxidation state coincide with that of the reaction rate.

In cases where sites can be differentiated by the IR spectra of an adsorbed reactant (see above), the step concentration change may be replaced by changing the isotopic label (e.g., $^{12}CO \rightarrow {}^{13}CO$) as the adsorption of the labeled compound is easily detected by a shift in wavenumber. Such extension of the SSITKA (steady-state isotopic transient kinetic analysis), which is typically used for studies on reaction mechanisms, by integrating structural and/or surface analysis techniques is nowadays established in many laboratories. For the reactions relevant for SCR, the pertinent studies are, however, still ahead.

The information given in this chapter demonstrates the complexity of research targeting the identification of active sites in real catalysts. The report on the state of insight into active site structures in SCR catalysts which will follow in the next sections should be seen on this background. This state of knowledge comes as a mosaic with contributions of many groups which are not necessarily consistent with each other. The picture is definitely transient, in some cases the details may well change by upcoming work with more powerful methods and with broader use of transient methods.

7.3 Supported Vanadia Catalysts

Supported vanadia catalysts promoted with tungsten oxide, sometimes with molybdena, are the industrial standard in SCR applications for stationary sources but have also been applied in urea-SCR schemes (cf. Sect. 2.1). In the following, the state of knowledge about the unpromoted V_2O_5/TiO_2 system will be discussed first, followed by some remarks regarding the role of the WO_3 promoter.

It has been known for long that the interaction of transition-metal oxides (V_2O_5, WO_3, MoO_3) with high surface area supports leads to the formation of monolayer surface oxide species up to a considerable coverage degree of the support surface (see, e.g., reviews [23, 40–44]). Silica is somewhat exceptional in this respect because of its low density of sites available for interactions with the supported oxide, therefore the following discussions are not valid for SiO_2 surfaces. The question whether the support surface becomes completely covered before the supported oxide starts to grow into the third dimension was subject to some

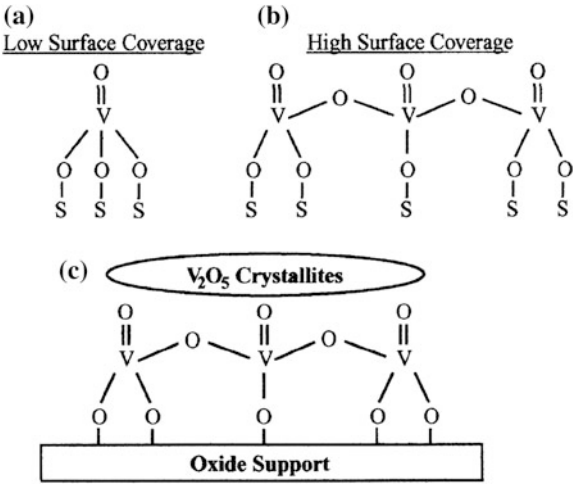

Fig. 7.5 Surface vanadium oxide species occurring on supported vanadium oxide catalysts. Reproduced from [42] with permission of Elsevier. **a** Isolated surface VO_4 species. **b** Polymeric surface VO_4 species. **c** Crystalline V_2O_5 nanoparticles above monolayer surface coverage

controversy [23, 41, 43–47]. Studies by the perfectly sensitive Ion Scattering Spectroscopy [48, 49] showed that in well-prepared catalysts the transition-metal (V or Mo) oxide species indeed cover the support completely in the dehydrated state before building second and third layers. Hydration of the fully covered surfaces results in some exposure of the support, apparently due to hydrolysis of the oxygen bridges to the latter with subsequent clustering of the supported species [43, 44]. Less optimized preparations involving ill-controlled deposition of precipitates may, of course, lead to different situations although the oxides have a tendency to spread over the support surface during heat treatments creating monolayer systems also under dry conditions. Indeed, for some systems (e.g., MoO_3/Al_2O_3) thermal spreading of the oxide onto the support surface is a practical alternative preparation route to aqueous techniques [50, 51].

It has been concluded from Raman spectroscopic studies that the TM oxide forms isolated surface oxide species at low coverages, which combine to two-dimensional oligomers with increasing coverage [23, 40–44]. Growth into the third dimension will result in relatively disordered clusters which can be, however, observed by Raman spectroscopy with high sensitivity, before ordered particles detectable by XRD are formed. On TiO_2, the vanadium in isolated species is tetrahedrally coordinated by oxygen with a short V=O bond and three longer bonds forming oxygen bridges to Ti atoms (Fig. 7.5). In the polyvanadates, some V–O–Ti linkages are replaced by V–O–V bridges, in addition, acidic V–OH groups may occur.

A recent EPR spectroscopic study [52] suggests some modification of this picture (Fig. 7.6). The catalysts were made by simple impregnation of a Ti

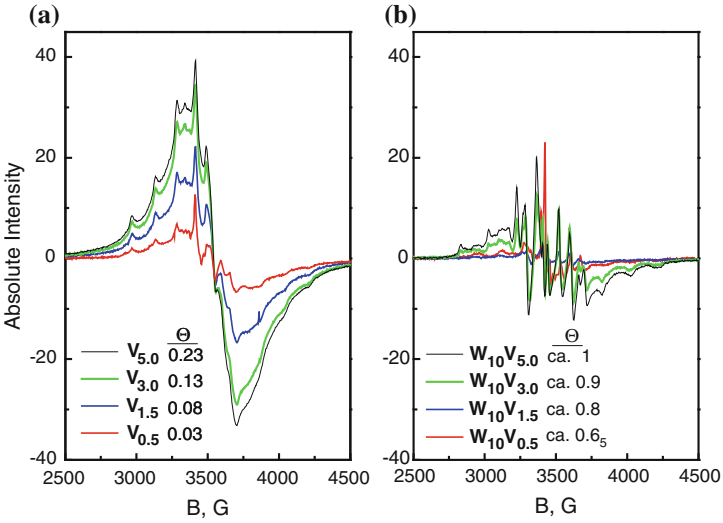

Fig. 7.6 EPR spectra of tungsten-free **a** and tungsten-containing **b** V_2O_5/TiO_2 catalysts after a reference calcination (623 K, 1 h), measured at 77 K. Spectra are normalized to the catalyst mass. Reproduced from [52] with permission of Elsevier

oxyhydrate with very high surface area resulting from the sulfate process, with subsequent calcination at a rather low temperature (623 K) with the intention just to fix the spontaneous speciation of V oxide structures on the surface. While the presence of three-dimensional clusters could be excluded by Raman spectroscopy, EPR showed a coexistence of isolated and oligomeric surface oxide species over a wide range of coverage degrees (Fig. 7.6a). The intensity ratio between the two signals present (multiplet—isolated sites, broad isotropic signal—sites in islands) confirmed the expected increased abundance of islands at larger V oxide coverages, but the clear detection of the isotropic signal at a V oxide coverage of <3 % suggests that surface vanadium oxide species have a much larger tendency to island formation on titania surfaces than so far assumed.

In the early literature, the vanadyl group (V=O) was thought to be the active site for the SCR reaction [53]. It was, however, soon observed that in catalyst series with varying composition the SCR rate grew stronger than linear with the vanadium content [54–57] as exemplified for V_2O_5/TiO_2 in Fig. 7.7. It was derived from the kinetic data that the polyvanadate-based sites in V_2O_5/TiO_2 would be an order of magnitude more active than the isolated sites [55]. From these observations, various proposals of binary sites with the O=V–O–V=O motif emerged, as reviewed, e.g., in [58]. At the same time, the relevance of Brønsted (V–OH) sites was concluded from IR and isotopic labeling studies [59, 60]. The well-known reaction mechanism by Topsøe (see Chap. 8), which was supported by IR spectroscopic and TPD studies [61–63] and became the basis of a successful microkinetic model of SCR over this catalyst type [64], indeed operates on a binary site containing an vanadyl and a V–OH group (O=V–O–V–OH).

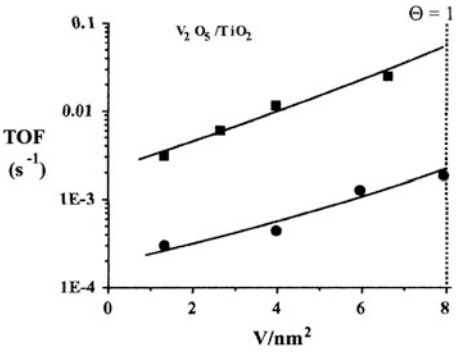

Fig. 7.7 Relation between density of surface V atoms in V_2O_5/TiO_2 catalysts and their activity for NH_3–SCR (•) and methanol oxidation (■) Reproduced from [42] with permission of Elsevier

On the other hand, the reality of SCR activity provided by isolated V oxide sites [55] has been supported by studies with vanadium-exchanged zeolites. A clear correlation between the intensity of the EPR signals of isolated $(VO)^{2+}$ ions and the reaction rate was found [65]. These sites obviously operate via a different, as yet unknown mechanism.

Several concepts were put forward to explain the promoting role of tungsten in V_2O_5–WO_3/TiO_2 catalysts. An increased surface acidity in presence of W favors the ammonia supply to the active site [66, 67]. Tungsten was observed to enhance the reducibility of the vanadia component [66, 68], which was explained by electronic interactions and was related to the observed increase of activity. An alternative approach considered the tungsten species just as competitors for the support surface, which force the surface vanadium oxide species to greater proximity and thus to the formation of the highly active binary sites [66] already at lower coverages. In this version, the surface tungsten oxide species are just spectators, the activities achieved in the promoted catalysts should be accessible without tungsten as well, but at lower BET surface areas. Tungsten is also known to favor the stability of the catalysts by delaying the sintering of the high surface area support.

The structure of surface tungsten oxide species was studied by Raman spectroscopy of monometallic WO_3/TiO_2 and of mixed V_2O_5–WO_3/TiO_2 catalysts [69]. Surface W oxide species are tetrahedrally coordinated ($(O)_3$–W=O) at low W content while strongly distorted octahedral sites ($(O)_5$–W=O) predominate on dehydrated surfaces at high W oxide coverage. These sites were found to coexist with tetrahedral monovanadate and polymeric surface vanadates in the mixed system. A trend to more polymeric surface V oxide species was observed with growing tungsten content, but no three-dimensional phase was seen even at total metal coverages which would significantly exceed the monolayer limit if both metals were to compete for the same surface sites [69]. No indications for bonds between surface W and V oxide species (W–O–V bridges) were reported.

In Fig. 7.6, the EPR spectra of the TiO_2—supported monometallic and mixed oxide catalysts are compared [52]. Surprisingly, the introduction of tungsten strongly suppressed the isotropic signal from the surface V oxide islands. The effect is drastic, because the coverages in the mixed systems are very high due to

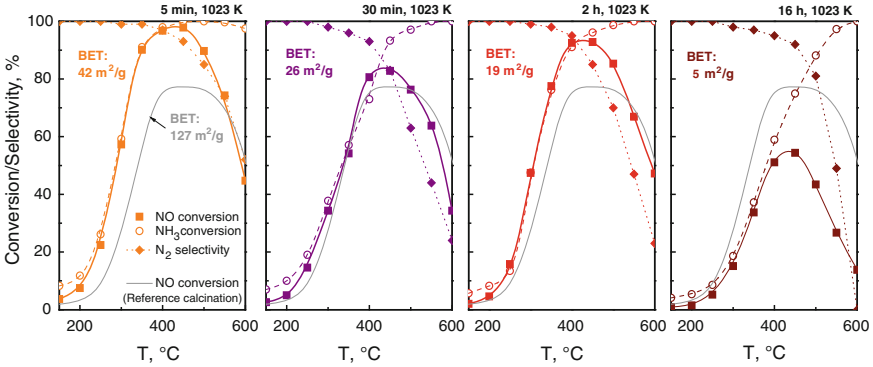

Fig. 7.8 Dependence of the SCR activity and selectivity of a V_2O_5–WO_3/TiO_2 catalyst (1.5 wt% V_2O_5, 10 wt% WO_3) on the duration of a calcination in air at 1023 K. Comparison with reference calcination (1 h at 623 K). From [70]

an intermediate calcination step which caused loss of surface area. For the catalysts containing 1.5 wt% V_2O_5, (…$V_{1.5}$), the isotropic signal almost completely vanished in presence of W although the total metal oxide coverage increased by an order of magnitude. Obviously, tungsten tends to break up island structures instead of favoring them. A complementary TPR study indeed suggested that most of the tungsten in these catalysts is in the vicinity of surface V oxide sites, not near W oxide sites [52]. Therefore, the promoting effect of tungsten is caused not by the formation but by the destruction of polyvanadate sites. Electronic interactions between W and V oxide species or a favorable influence of W on surface acidity would comply with this picture, but also a dependence of the specific activity of the active (V–O–V) sites on the size of the island in which they are contained, the smallest size offering the highest activity.

These alternatives were further differentiated by a study of the catalyst response to high temperatures [70]. Mixed oxide systems were found to activate strongly upon treatment at high temperatures in oxidizing medium (Fig. 7.8). Two activity peaks can be seen with increasing treatment duration at 1023 K (panels a and c) and concomitant decrease of the BET surface area. Under other calcination conditions, even a third activity maximum emerged. While the details of these phenomena are not yet fully understood, we found clear evidence from several methods (Raman spectroscopy, XRD, TPR) that the decrease of the support surface area causes the tungsten oxide species to segregate from the surface, not the vanadium oxide species. Therefore, the drastic activation effect seen in Fig. 7.8 is most likely related to a growth of surface V ensembles at places where the tungsten loses contact with the surface. This is incompatible with both the concept of electronic interactions between W and V oxide sites and of acidity effects determining the activity trends. Instead, it seems to indicate that the spontaneous arrangement of W and V oxide species on the titania surface leads to an excessive isolation of vanadium oxide sites. This is relaxed by segregation of W oxide

species from the surface under thermal stress, which allows for more highly active dimeric sites. Under heavy thermal stress, the surface vanadia phase remains two-dimensional while the tungsten oxide forms large WO_3 crystals. The poor performance resulting under these conditions suggests a lower activity of V–O–V dimer sites when they are part of large islands.

7.4 Zeolite-Based Catalysts

Zeolites are unique among catalyst supports in many aspects, e.g., in the availability of well-defined, energetically nonequivalent cation exchange sites. The expectation that cations exchanged into zeolites will all end up in these sites seems to be fulfilled, however, only for monovalent ions. SCR-related research has much contributed to the insight that exchange of polyvalent cations may result in complicated species distributions, probably due to the extra-lattice oxygen introduced into the system for charge neutralization.

7.4.1 Fe Zeolites

The discussion of active sites for NH_3–SCR has been much influenced by structural data collected in earlier studies related to the SCR with hydrocarbons (HC–SCR). For the same reason, the discussion has long been focused on the ZSM–5 matrix although different zeolites, in particular zeolite Beta, meanwhile seem to be more promising for technical application. The early studies dealt with over-exchanged samples (Fe/Al = 1, corresponding to $\approx$5 wt% Fe at an Si/Al ratio of $\approx$15), which were first described by Feng and Hall [71] and could be reproducibly prepared by chemical vapor deposition (CVD) of $FeCl_3$ into H–ZSM–5 as reported by Chen and Sachtler [36]. These authors proposed that the iron which is atomically dispersed in the form of Z–O–$FeCl_2$ species after the CVD step, rearranges quantitatively or to a large extent into dimeric species held together by an oxygen bridge (Fe–O–Fe) after washing and calcination [36, 72]. This view was supported, e.g., by the partial reappearance after calcination of the IR band of Brønsted OH groups, which had been completely quenched by the CVD step, and by the easy (stoichiometric) oxidation of CO to CO_2 by these samples, which suggests the vicinity of two Fe atoms accommodating the two electrons transferred. The assignment of the high HC–SCR activity of these catalysts to the binuclear Fe–O–Fe sites was encouraged by analogies with the active structure in the enzyme methane monooxygenase [73] and by previous analogous assignments of activity in NO decomposition and HC–SCR to analogous Cu–O–Cu species in Cu–ZSM–5 [74].

Several groups investigated over-exchanged Fe–ZSM–5 by X-Ray absorption spectroscopy and supported unanimously the formation and catalytic relevance of the binuclear Fe–O–Fe sites [75–77]. The EXAFS spectra obtained in these studies

were successfully analyzed by models yielding coordination numbers near or equal to one for the second coordination shell (Fe–Fe). A note of caution was given by Marturano et al. [77] who found by magnetic measurements that the antiferromagnetic coupling, which is expected between the Fe atoms in binuclear sites, was not complete. Despite 30 % of the iron detected as isolated ions, the EXAFS data were still discussed in terms of predominating binuclear sites.

On the other hand, Heinrich et al. obtained Fe–Fe coordination numbers below 1 in their EXAFS analysis of over-exchanged Fe–ZSM–5 subjected to different calcination regimes [37]. Supported by the observation of a significant amount of large clusters (particles) by Moessbauer spectroscopy (cf. Fig. 7.4) they concluded that EXAFS coordination numbers can be only averaged quantities in these materials and thus identified the presence of significant amounts of isolated Fe oxo sites in their zeolites. As the SCR activities of these catalysts were comparable with those of other groups which claimed considerably less particle formation and predominant presence of binuclear Fe–O–Fe sites in their samples [36, 78], Heinrich et al. assigned the (HC-)SCR activity to sites which would be minority species in all catalysts compared, e.g., isolated sites [37]. This assignment was strongly supported by the observation of attractive SCR activity of a sample containing just 0.5 wt% Fe [79]. This catalyst, which was prepared by a different method, did not exhibit any significant Fe–Fe scattering signal in EXAFS which might have indicated binuclear Fe–O–Fe sites.

In the following, the heterogeneity of the Fe speciation in over-exchanged Fe–ZSM–5 has been confirmed by other groups as well [80] although in the mean time, >70 % of the iron had been claimed to be part of Fe–O–Fe pairs in catalysts that contained >45 % of the iron in large (2–10 nm) particles according to the Moessbauer spectra [81]. Heijboer et al. found that the EXAFS spectra of over-exchanged Fe–ZSM–5 cannot be unambiguously analyzed [80]: they presented models including next nearest Si(Al) neighbors that represent the data equally well as those published earlier [81] and resulted in much lower Fe–Fe coordination numbers (see also Pirngruber et al. [82]). Likely structures of Fe species in ZSM–5 are illustrated in Fig. 7.9, which cites molecular modeling results given in [80]. These models should be taken just as examples: EPR spectroscopy identifies, for instance, at least three different isolated sites ([30, 83], see also Fig. 7.3), which have been related to the α, β, und γ cation exchange sites meanwhile [84]. The binuclear site is nowadays rather lumped into the oligomers, which can be identified by UV–Vis signals in a particular wavelength range [30, 85]. Upon calcination, the Fe species tend to migrate toward the external surface and to aggregate still in the zeolite [37, 81], which is nicely demonstrated by TEM–EDX images from [81] and TEM images from [86] in Fig. 7.10a–c. The wavelength region related to these species in the UV–Vis spectra differs from those of the oligomers although it has remained unclear which aggregation degree would cause the wavelength shift observed [30, 85]. Finally, oxide or oxihydrate crystals segregate from the zeolite (Fig. 7.10b). The migration is favored by moisture, the intra-zeolite particles most likely destroy and include part of the zeolite structure which explains their invisibility by XRD and EXAFS (see Fig. 7.4).

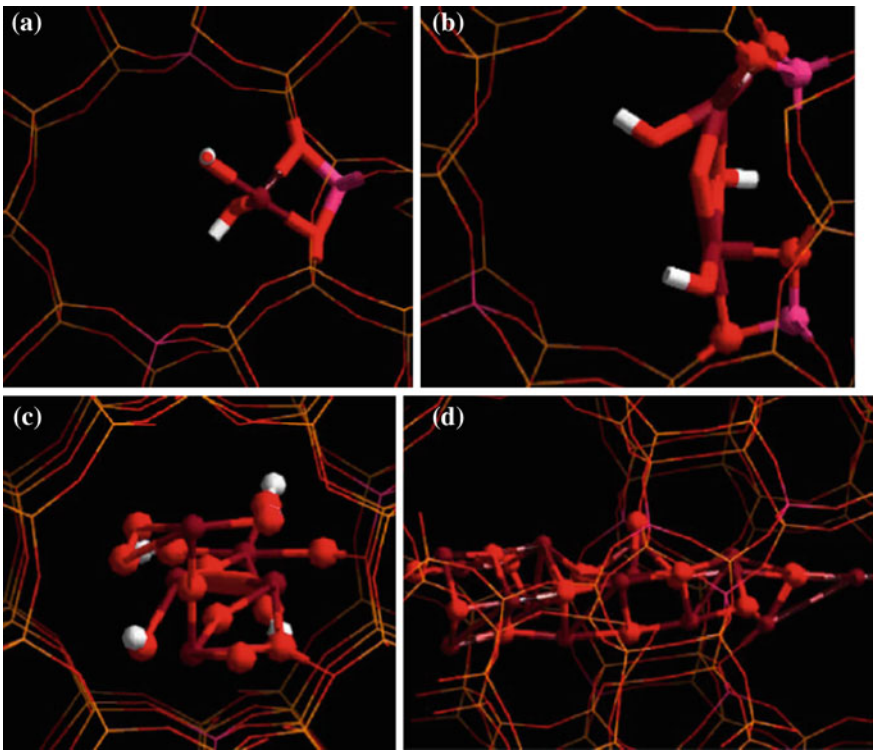

Fig. 7.9 Molecular models of Fe oxo species in zeolites. **a** mononuclear Fe oxo site, dehydrated; **b** binuclear Fe (hydr)oxo site, **c**, **d** oligomeric Fe oxo sites of different nuclearities in straight channel, seen from different sides. Framework represented by *thin lines*, atoms in extra framework species by balls: *red*—O, *pink*—Al, *dark red*—Fe, *white*—H. From [80] with permission of Elsevier

Due to the complexity of over-exchanged Fe–ZSM–5, the subsequent studies were undertaken with ZSM–5 containing small amounts of iron, and NH_3–SCR was included owing to its upcoming technological relevance. UV–Vis and EPR spectroscopy became the most important analysis techniques at the expense of EXAFS because of their potential to differentiate coexisting Fe species [30]. For a series of samples prepared by a special ion exchange technique (cf. [83]) activity in both SCR reactions was correlated with the abundance of Fe sites derived from a quantitative analysis of the UV–Vis spectra, neglecting a possible wavelength dependence of the extinction coefficient [86].

For HC–SCR, this correlation resulted in strong support for a contribution of both isolated and oligomeric Fe oxo sites to the reaction rates observed at low temperatures. At high temperatures, the oligomers catalyze the oxidation of the hydrocarbon reactant very effectively, therefore, the best catalysts for HC–SCR contain iron only in small quantities. The results for NH_3–SCR are summarized in

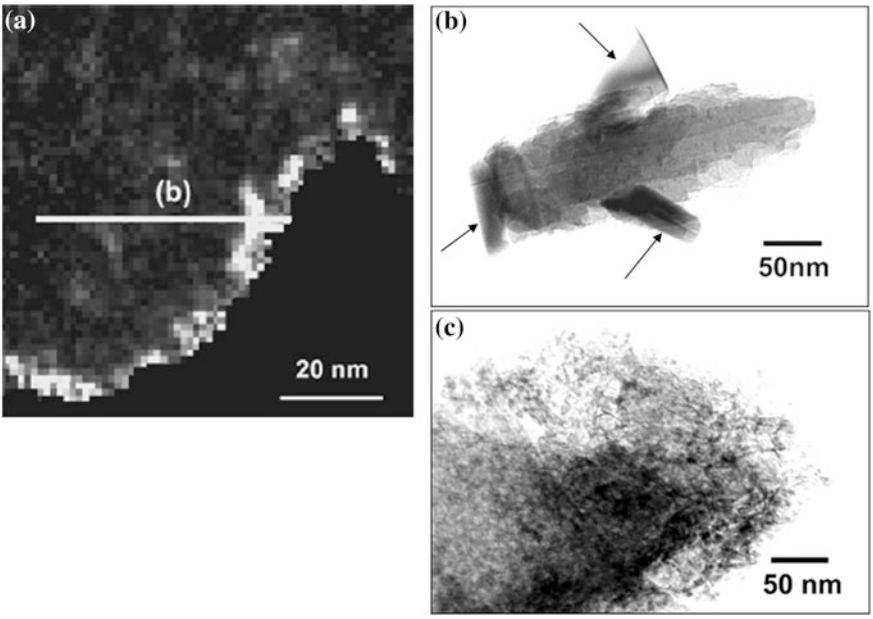

Fig. 7.10 Electron microscopy images of Fe–ZSM–5. **a** STEM/EELS micrograph (Fe/O map) of over-exchanged Fe–ZSM–5 after calcination with extremely slow temperature gradient [81], line scan along *line* (**b**) not shown; **b** crystallites on over-exchanged Fe–ZSM [86], **c** Fe enrichment in Fe–ZSM–5 of low Fe content (1.2 wt%)

Fig. 7.11. Surprisingly, the correlation with the total Fe content was superior even to that with the sum of oligomers and isolated sites, which was explained with the irregular structure of the intra-zeolite "particles" (cf. Fig. 7.10a, c) offering a non-negligible surface area available for catalysis. Unlike in HC–SCR, the oxidation of the reductant is much less pronounced in NH_3–SCR over Fe–ZSM–5, therefore, the oligomers can be tolerated in the catalysts. Rather, from the course of the NO conversion curves with increasing Fe content it was proposed that the oligomers may even contribute more strongly to the total reaction rate at higher temperatures than under the conditions for which the correlation (Fig. 7.11) was made [86]. From this, the best catalysts for NH_3–SCR would contain large amounts of iron in the highest possible dispersion.

The surprisingly good correlations between site abundance and SCR activity still leave a number of questions unanswered. As already mentioned, "isolated sites" is a quantity lumped of at least three species detectable by EPR. The redox properties of these sites in the typical feeds (NH_3–SCR and HC–SCR) were found to be very different, octahedrally/distorted tetrahedrally coordinated isolated sites being more prone to reduction than tetrahedrally coordinated sites under conditions where oligomers withstood reduction completely [87]. As SCR most likely requires Fe to be in the +3 state in order to activate the reductant (cf. Chaps. 8 and 9),

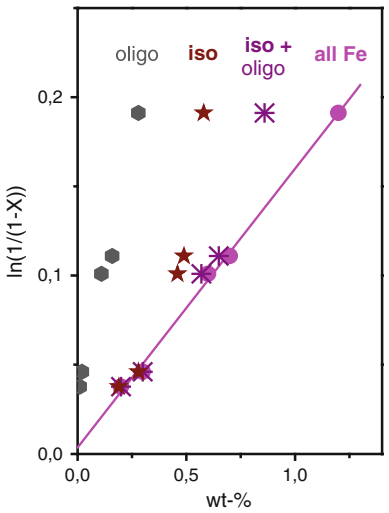

Fig. 7.11 Correlation of the rate constant of NH_3–SCR at 523 K with the abundance of different site types in Fe–ZSM–5 assessed from UV–Vis spectra. From data in [86]

the contribution of these sites to the observed activity should be different. The marginal influence of these differences on the quality of the correlations discussed above may arise from a low degree of variation in the concentration ratios between these sites in our series of samples. Likewise, the "oligomers" comprise a distribution of oligomerization degrees. The small NH_3 oxidation activity found with Fe–ZSM–5 arises from clustered phases, from the oligomers rather than from the particles. When we used a Fe–ZSM–5 catalyst after ≈ 2 years storage under the same reaction conditions as before, we observed the influence of ammonia oxidation on the conversion-temperature curves to be larger than in the earlier measurements (see [86, 88]) although we could not relate this to significant changes in the UV–Vis spectra. Maybe an influence of the oligomer size on ammonia oxidation activity remains to be discovered here. Finally, it has been proposed that the UV absorption of binuclear sites may fall into the wavelength region typical of isolated sites if their antiferromagnetic coupling is weak (hydroxo-bridged dimers) [82]. In our UV–Vis studies, no significant differences occurred between measurements of a calcined sample stored subsequently at ambient or in situ right after calcination, therefore, we do not consider the hydroxylated binuclear site relevant for our assignments.

The sites active for NH_3–SCR in Fe zeolites have been addressed in a number of other, mostly more recent studies, which did not result in convergent conclusions. Based on EPR measurements, Long and Yang [83] assigned activity for NH_3–SCR exclusively to tetrahedrally coordinated isolated sites cooperating with Brønsted siteds. Exclusively isolated sites were also considered responsible for NH_3–SCR by Krishna and Makee [89] and by Doronkin et al. (Fe-Beta [90]). Opposed to this, Klukowski et al. suggested a dual site mechanism for Fe-Beta where NH_3 and NO are activated at neighboring Fe^{3+} sites, and admitted only a minority role for a possible single-site mechanism [91]. The dual site may be part

of oligomers or consist of two nearby isolated Fe^{3+} ions. Iwasaki et al. proposed NO_2 TPD as a most useful tool for the elucidation of active sites as its high-temperature peak appears to correlate with activity in NH_3–SCR [92]. This peak was associated with "oxo-Fe^{3+} at ion exchange sites" [92, 93] which includes, however, binuclear sites as far as both Fe ions are related to framework Al cations. In a more recent article, the binuclear sites were described as a subcategory of oligomeric sites [94], which shifts the assignment closer to that of Schwidder et al. [86]. Sobalik and coworkers have recently stressed the significance of the Al distribution in the zeolite framework for the active site structure, a motive which has been developed by scientists of the Prague Heyrovsky institute over years and has been recently reviewed in [95]. In this concept, close Al framework sites in opposite positions of a six-ring stabilize Fe^{2+} ions without extra-lattice oxygen, while single Al framework sites are coordinated with Fe^{3+} oxo species. The latter are considered responsible for the activity in NH_3–SCR [96].

The conflicting conclusions mentioned arise at least partly from the limited potential of the available analytical methods for analysis of the complex site structure in Fe zeolites. In this situation, the group of O. Kröcher resorted to a statistical approach in which the distribution of the Fe sites was assumed to follow a (random) distribution of Al in the zeolite framework, and the formation of bi, tri, and polynuclear structures was assumed to occur when nearby Fe sites are located within certain distances [97, 98]. The site abundances obtained on this basis, which were validated by comparison with UV–Vis spectra of a samples series covering a wide range of Fe contents [98], were used to explore correlations within a large body of very accurate rate measurements at different temperatures [99]. From this, Brandenberger et al. concluded that the catalytic reaction rate results exclusively from isolated sites at low temperatures while oligomeric structures contribute at higher temperatures, which agrees to some extent with the picture proposed in [86].

The importance of acidity for NH_3–SCR has been discussed also with respect to Fe zeolite catalysts. A favorable role of acidity is á priori plausible because this tends to increase the local concentration of the ammonia reductant near the active sites. The more fundamental question is, however, if an acidic function is part of the active sites as, for instance, in the sites driving the reaction cycle proposed by Tøpsoe [61–63] for V_2O_5/TiO_2 catalysts. From a comparison of SCR activities measured with Fe in nonacidic and acidic zeolite supports, Schwidder et al. concluded that acidity favors the reaction without being an essential ingredient of the active site and hence the reaction mechanism [100]. A more recent study of Brandenberger et al. arrived at similar conclusions [101], which are at variance with some earlier proposals, e.g., in [83].

The technical relevance of Fe zeolites is related to their potential to catalyze the fast SCR reaction (Eq. 7.2) rather than to their activity in standard SCR. Fast SCR is a rather facile reaction which has been proposed to proceed without any involvement of Fe sites [102, 103]. This has been confirmed in [88], but it has been shown at the same time that Fe zeolites offer sites which accelerate the reaction dramatically. Standard SCR and fast SCR are stoichiometrically related to each other: The former (Eq. 7.1) results when NO oxidation (Eq. 7.3) is added to fast SCR (Eq. 7.2).

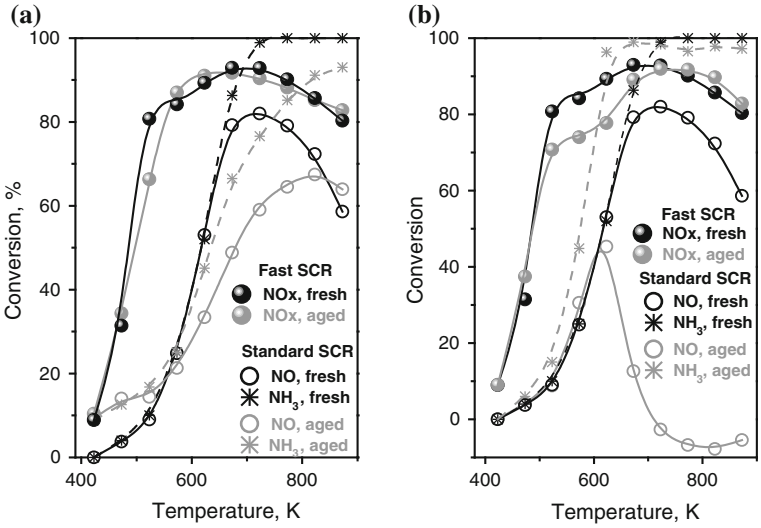

Fig. 7.12 Deactivation of an Fe–ZSM–5 catalyst in standard and fast SCR. **a** aging in moist atmosphere, 10 vol% H_2O in air, 923 K, 48 h, **b** aging in presence of water and SO_2, 5 % H_2O, 200 ppm SO_2 in He at 823 K over 65 h. 1,000 ppm NO, 1,000 ppm NH_3, 2 % O_2 in He, 750,000 h^{-1}, NOx being NO (standard SCR) or an equimolar NO/NO_2 mixture (fast SCR). From [88] with permission of Elsevier

It has been proposed that this relation holds also for the reaction mechanism of standard SCR, with NO oxidation as rate-determining step followed by the very fast reaction of the resulting NO/NO_2 mixture according to Eq. (7.2) (see Chap. 8, earlier work summarized in [97]). This view implies that the active sites of NO oxidation and of standard SCR are identical while those of standard and fast SCR might be different.

The latter has been indeed reported in a study by Schwidder et al. [88] where the activity for fast SCR was found to survive hydrothermal stress and impact of SO_2 much better than that for standard SCR (Fig. 7.12). From the observation that fast SCR was effectively catalyzed by a sample containing just 0.2 wt% Fe, according to UV–Vis and EPR spectroscopy almost exclusively as isolated sites and that more iron, be it as isolated, oligomeric, or particulate species, did not result in significant improvement, it was concluded that fast SCR is catalyzed by a sub-entity of the isolated sites. In recent *operando* EPR studies, Fe sites in β and γ positions remaining in the 2+ state during calcination but being oxidized to Fe^{3+} in presence of NO_2 have been identified as candidates [104].

In another recent study, it was attempted to change the fractional occupation of the ZSM–5 cation sites by the Fe species by loading the zeolite previously with different amounts of Na or Ca ions [105]. The subsequent introduction of the Fe component (ca. 0.25 wt%) was accomplished by a dry method (solid-state ion exchange) to avoid leaching of the co-cations. Figure 7.13 shows conversion

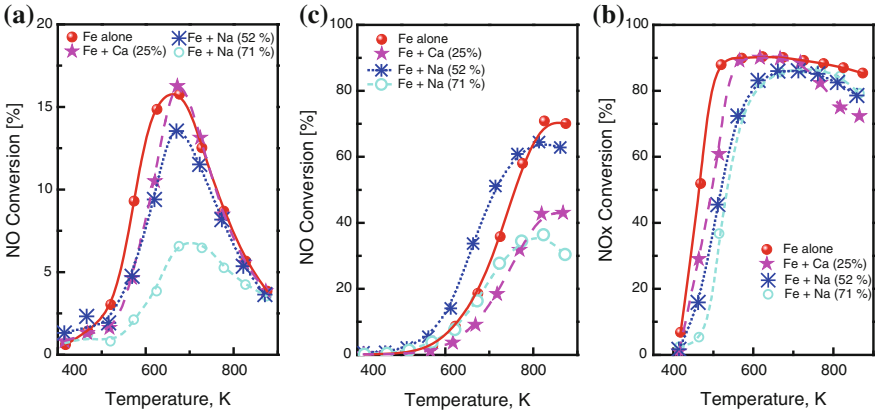

Fig. 7.13 Influence of inactive co-cations (Ca, Na, at different exchange degrees) on the catalytic properties of Fe–ZSM–5. **a** NO oxidation, **b** standard SCR, **c** fast SCR. From data in [105]

curves measured with these catalysts in the three relevant reactions (7.1) through (7.3). These curves demonstrate clearly that the active sites dominating the catalytic behavior are different for all three reactions. Thus, activity for standard SCR was improved by the presence of Na ions (ca. 50 % exchange degree) as compared to the Fe-only sample (Fig. 7.13b), while the activity for the other two reactions was deteriorated (Fig. 7.13a, c). This is another piece of evidence rejecting that standard SCR proceeds via a sequence of NO oxidation to NO_2 and fast SCR. The differences between NO oxidation and fast SCR are less striking but still pronounced (Fig. 7.13a, c): Thus Fe–ZSM–5 preoccupied with Ca or with Na (exchanged to 50 %) behave very similar in NO oxidation but clearly different in fast SCR. A further increased Na exchange degree leads to a strong deactivation in NO oxidation whereas in fast SCR, a loss in performance occurs only at low temperatures. The differences in the active site structure causing the activity changes depicted in Fig. 7.13 are subject to ongoing characterization work.

To summarize, there is no generally accepted view on the active sites responsible for the reactions relevant for NOx reduction in Fe zeolites. Several studies suggest a participation of all Fe sites accessible from the gas phase, which agrees with the observation that considerable SCR activity has also been reported for Fe oxide on open supports, e.g., tungsten-promoted $FeOx/ZrO_2$ [106], but correlations with exclusively isolated Fe sites have also been claimed. Research targeting the identification of the sites active for fast SCR has only just commenced. While it is clear that this reaction is catalyzed by a very stable isolated minority site, a recent *operando* EPR study supported by Moessbauer data suggests that this site may be in the Fe^{2+} state in a calcined catalyst and can be oxidized to Fe^{3+} only by NO_2 [104]. Fe ions stabilized by close Al sites in the framework as proposed by Dedecek et al. [95] might be candidates for that. Still, there is not as yet a well-established relation between the reaction mechanisms of

SCR (standard and fast) over these catalysts and the candidate sites because the mechanistic discussion was long dominated by the assumption of NO oxidation being rate determining for standard SCR, and more recent concepts still need to be related to the knowledge about the site structure in Fe zeolites.

7.4.2 Cu Zeolites

As mentioned above for Fe zeolites, the discussion on active sites in Cu zeolites has long been based on results obtained previously in research on HC–SCR, in the case of copper also on NO decomposition. The early work on all these reactions was reviewed in [107]. Actually, the activity of Cu zeolites for NH_3–SCR was discovered earlier than that for HC–SCR (NO/NH_3 reaction over Cu–Y—1975 [108, 109]; HC–SCR—1989/90 [110, 111]), but as the reaction was performed without oxygen in the feed, Cu(II) became reduced at rather low temperatures which quenched the reaction. $[Cu(NH_3)_4]^{2+}$ complexes were considered to be the active sites [112].

Cu–ZSM–5 was the system for which the phenomenon of over-exchange was first described [110]. For NO decomposition, a steep increase of the turnover frequency around 100 % exchange degree [110, 113, 114], the conclusion that the active sites are a minority which easily interchanges between the +2 and +1 oxidation states under reaction conditions [114, 115] and the identification of such sites with binary Cu–O–Cu species [116] suggested a particular role of aggregated entities in this reaction. There was disagreement with respect to the structure of these aggregates already with the copper zeolites, where binuclear (Cu–O–Cu) sites were advocated by the majority of groups [110, 115–118] while some groups proposed the formation of small intra-zeolite oxide clusters (oligomers) [119, 120]. The latter was supported by the observation of very strong enrichment of copper in the XPS sampling region of freshly prepared Cu–ZSM–5 without any indication for the formation of massive phases [120], which would have been sensitively detected by the help of the Auger parameter [120–124]. Indeed, redox treatments decreased the copper excess in the external surface region, apparently by decomposition and redistribution of the copper oxide oligomers over the whole zeolite crystal [120].

While the beneficial role of overstoichiometric Cu is obvious for NO decomposition, there are diverging reports with respect to HC–SCR. Observations of peak activities at exchange levels slightly above 100 % [125–127] were considered to indicate a particular activity contribution of Cu–O–Cu sites or clusters, but results depended on the type of hydrocarbon reactant and on the reaction conditions. A completely different explanation given by Wichterlova et al. [128] is based on the concept of the active sites being influenced by the Al framework distribution [95]. From work with luminescence and IR spectroscopy (adsorbed NO), two different types of isolated Cu ions were differentiated: one, which predominates at low Cu content, is change-balanced by two nearby framework Al ions, the other one, which carries extra-lattice oxygen, is formed only at higher Cu

content and was identified as the active site for NO decomposition. HC–SCR and NH_3–SCR were proposed to require the cooperation of both kinds of Cu ions. Ciambelli et al. found the normalized reaction rates (per Cu atom) of HC–SCR to increase up to full exchange, but then to decrease markedly [127], which calls into question the relevance of excess copper. In a study of propene-SCR with copper chloride species introduced into Na–ZSM–5 by dry methods (i.e., as guest species), normalized reaction rates were found to be of the same order as in usual SCR catalysts, which suggests that excess copper is just another site type for hydrocarbon-SCR, but without particular merits [121]. This is in agreement with the observation that Cu zeolites which differed strongly in NO decomposition activity exhibited less differences in HC–SCR [129].

The study with Cu chloride species hosted in Na–ZSM–5 [121] showed at the same time that HC–SCR with the reductant propene is possible without Brønsted acidity, which had been under debate as well (cf. [130–135]).

In studies with the ammonia reactant, the coexistence of isolated and binary sites was a major topic as well. In a kinetic investigation of NH_3–SCR over Cu–Y catalysts of different Cu content, Kieger et al. [136] found the turnover frequency (rate per Cu atom) to increase significantly with the copper content at low reaction temperatures while the trend was weaker above 600 K. Based on characterization by temperature-programmed reduction and reoxidation, TPD of ammonia and IR of adsorbed NH_3, the authors assigned the selective reaction observed at low temperatures to Cu–O–Cu sites which form in supercages at high copper content while analogous binary sites in the sodalite cages were considered responsible for the relatively intense N_2O formation under these conditions. Above 600 K, where the N_2O selectivity decreased markedly, all accessible copper was proposed to catalyze the selective reaction. Komatsu et al. likewise suggested a crucial role of binary Cu–O–Cu sites from kinetic studies of NH_3–SCR in Cu–ZSM–5 of varying Cu content [137]. The proposal of Wichterlová et al. according to which a cooperation between two different Cu ions is required for NH_3–SCR ([128], see above) sounds similar, but it does not invoke an oxygen bridge between them because one Cu ion is change-balanced by two framework Al ions.

The renewed interest in Cu zeolite catalysts for NH_3–SCR after the discovery of high activity, selectivity, and stability of Cu chabasite materials has led to a number of studies aimed at the elucidation of the active site in this zeolite. It has been reported that Cu ions are present in just one single crystallographic position in these catalysts. This was concluded from Rietveld refinement of XRD data, and the Cu ion was found within the cage just outside the double-six rings connecting the zeolite cages [138]. The relevance of this site for NH_3–SCR was shown in subsequent work [139, 140]. Deka et al. [141] derived similar conclusions from operando-XAFS measurements, where the detailed coordination geometry could be resolved more accurately due to the local sensitivity of EXAFS. A model of the site at different temperatures is shown in Fig. 7.14 where it can also be seen how NH_3 adsorbed onto the Cu ion at low temperatures attracts it slightly toward the center of the cage. It should be noted that this view has been challenged by Kwak et al. on the basis of TPR and IR (CO and NO probe molecules) data, according to

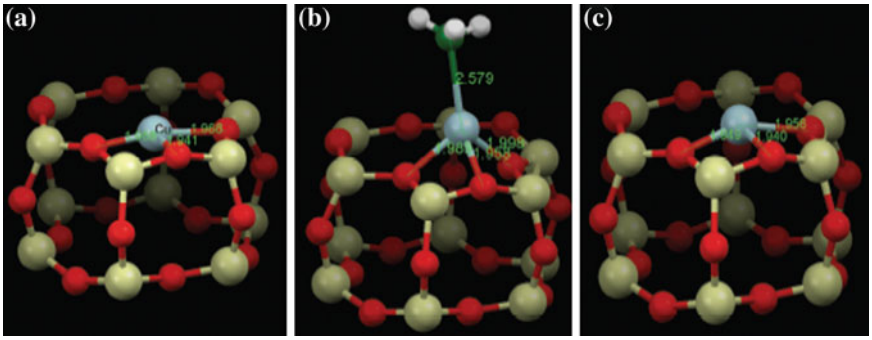

Fig. 7.14 Illustrations of the local copper environment in d6r subunit of CHA. **a** Local structure after calcination, with copper in the plane and slightly distorted from the center of the d6r subunit of CHA; **b** interaction with NH_3 at 423 K under SCR conditions resulting in a coordination geometry change; **c** under SCR conditions above 523 K. From [141] with permission from the American Chemical Society

which a second cation position is populated already at 40 % Cu exchange level [142]. The additional position, which is located more into the cage, but also coordinated to a six-ring, provides a higher redox activity to the Cu ion. Irrespective of the outcome of this controversy, it seems that the activity of Cu–SSZ–13 arises from isolated sites. This very stable activity is very much the same as the one which other Cu zeolites (e.g., Cu–ZSM–5) [143], the performance of which was described to be dominated by binary Cu–O–Cu species in earlier studies [137], can provide only in the fresh state.

7.5 Recent Catalyst Development

In recent years, much work has been devoted to the search for alternative oxide catalysts for NH_3–SCR, and from the characterization work included in these studies, conclusions regarding the active sites have often been drawn. The most promising systems are based on the elements manganese and cerium, which are often combined with other elements or deposited on supports (see Sect. 2.4).

The extremely high activity of bulk manganese oxides, which provide very large reaction rates at temperatures below 470 K, can apparently arise from several oxidation states of Mn [144–146]. It was shown that MnO_2 is the most active phase, however, its labile oxygen favors the oxidation of ammonia to N_2O [146] while Mn_2O_3 offers significantly better selectivity for N_2 at lower reaction rates [145, 146]. The sizeable N_2O formation over these catalysts and their low thermal stability has prompted efforts to stabilize their active sites on supports or by creation of mixed oxide phases.

Carbon-supported Mn oxides show similar activities as unsupported samples. On the basis of XPS evidence, Yoshikawa et al. concluded that the Mn oxidation state on their surface is +3 [147]. At the same time, Grzybek et al. [148] were

skeptical about the potential of XPS to reliably differentiate Mn^{3+} and Mn^{4+}—at least in routine application (see below). They stated that there may be oxide crystals and two-dimensional layer structures on the carbon surface, where the crystals are more active, whereas the monolayer structures are more selective toward N_2 [149].

Observations made with MnOx supported on other materials are somewhat different. No bulk phases can be observed on them at low Mn loadings, but the bulk oxides (e.g., Mn_2O_3) appearing at high Mn content did not improve the activity [150]. It was proposed on the basis of a multitechnique characterization study that Mn is present on TiO_2 in the form of monomeric surface oxide species at low Mn loading and as oligomeric monolayer structures upon increase of the Mn content [151]. Above the theoretical monolayer coverage, amorphous oxide layers are formed first whereas crystalline structures appear only at rather high Mn loadings. On the basis of XPS measurements, Pena et al. identified Mn^{4+} and Mn^{3+} on their Mn/TiO_2 catalysts and concluded a larger activity of the former from the catalytic behavior of the samples investigated [152]. Analogously, Mn^{4+} was considered the most active oxidation state by Zhuang et al. [153]. The latter authors observed a pronounced dependence of the activity on the Mn surface density on TiO_2 and concluded that the activity contribution of Mn^{4+}–O–Mn^{4+} sites exceeds that of isolated Mn^{4+}–O–Ti groups. This agrees with mechanistic proposals of Marban et al., which operate with binary Mn–O–Mn sites [154, 155]. Marban et al., however, proposed the Mn oxidation state to be +3 in these sites, and the mechanism involves a redox cycle between Mn^{3+} and Mn^{2+} in agreement with earlier concepts derived for Mn/Al_2O_3 catalysts [156–158]. Mn^{3+} was also advocated as the most active state by Yoshikawa et al. [147] and Li et al. [159].

The disagreement with respect to the active oxidation states is most likely related to the problem that the Mn oxidation states are not easily differentiated by XPS. Due to multiplet splitting, the 2p lines of many 3d elements are broad and asymmetric, and it is inappropriate to fit them with symmetric line profiles. The problem has been nicely illustrated by Biesinger et al. recently [160]. Moreover, binding energies of reference compounds for Mn^{3+} and Mn^{4+} (γ-Mn_2O_3, MnO_2) are within just 1 eV [148], which would be challenging even with well-behaved line profiles. Therefore, Mn 2p XPS, which is exclusively used by most of the authors, is not an appropriate tool for the discrimination between Mn oxidation states [148, 149]. Instead, the splitting of the Mn 3s signal (also by the multiplet effect) gives better evidence for the oxidation state(s) present [161], however, due to the rather weak intensity of this signal it has been rarely measured with supported catalysts.

Mixed oxides of manganese with other elements, e.g., with Fe [162] often exhibit much better thermal stability and selectivity to N_2 at only slightly diminished activity (compared with pure Mn oxides). The improved properties have been attributed to Mn–O–M (M=Cr, Fe, Ce) linkages [163–165], and thermally stable stoichiometric compounds ($CrMn_{1.5}O_4$ [163], $Fe_3Mn_3O_8$ [164]) have been proposed to be active in these mixed-oxide catalysts. The redox chemistry would then be distributed between two redox elements.

Cerium is another redox element successfully applied in alternative catalysts for NH_3–SCR. It offers promising nitrogen selectivity and stability though at somewhat lower activity. To exhibit these properties, Ce has to be deposited onto supports, because the pure oxide is rather inactive unlike the Mn oxides. Apparently, the bridging bonds between Ce and different elements (Ce–O–Ti in case of TiO_2) are important for SCR catalysis. This has been the rationale to develop very interesting Ce/TiO_x mixed oxide catalysts by homogeneous precipitation [166, 167]. In [167], the Ce–O–Ti linkages were even detected by XAFS. Likewise, Ce–O–W bridges have been considered responsible for promising properties of CeO_2–WO_3 coprecipitated catalysts [168]. Little is known about the most favorable active oxidation state of the Ce cation. While the Lewis acidity of Ce^{4+} has stressed in [168], the same authors considered the increased Ce^{3+} surface concentration (compared to CeO_2) favorable because of a concomitant formation of Brønsted sites [169].

7.6 Concluding Remarks

Research on heterogeneous catalysts is very much driven by the desire to identify the active sites for useful reactions. The combined catalytic and characterization work required for this generates an experimental basis and useful ideas for further catalyst improvement. From such work, it appears that the SCR of NO by NH_3 can proceed on different site types over the most important catalysts known. For vanadium-based systems, there is general agreement that binary V–O–V moieties including a Brønsted site are the most active structures, and a well-accepted mechanism is available for this site. At the same time, isolated $(VO)^{2+}$ ions exchanged into zeolites can catalyze the same reaction, apparently via a different mechanism. According to recent studies, the W promoter creates an optimum degree of isolation for the TiO_2-supported binary V–O–V sites, which appear to lose their reactivity when they are incorporated into large surface oxide patches.

For Fe- and Cu-modified zeolites, there is general agreement that NH_3–SCR can proceed on isolated cation sites, but their intrinsic activities appear to depend in an unknown way on the cation position in the zeolite. There are indications for the involvement of oligomeric oxide structures in catalysts as well although this is not generally accepted. Fast SCR over Fe zeolites uses exclusively isolated sites, probably a type stabilized as Fe^{2+} by two nearby framework Al ions.

Active site concepts for Mn- and Ce-based systems are not yet well developed, which is partly due to problems in the reliable differentiation between oxidation states in case of Mn.

Acknowledgments I would like to acknowledge a fruitful cooperation with all coauthors of own publications cited in this chapter, and for the funding by the German Science Foundation (DFG), by Interkat GmbH, Königswinter, Germany, and by Crenox (now Sachtleben Pigments, Krefeld, Germany). I am particularly grateful for the many years of inspiring exchange of ideas, materials, and results with Prof. Angelika Brückner, LIKAT Rostock, Germany. Finally, I want to thank my actual PhD students Inga Ellmers, Mariam Salazar Rodriguez, and Rosemary Fowler for support by literature work and proof reading.

References

1. Taylor HS (1925) A Theory of the Catalytic Surface. Proc Royal Soc A 108:105–111
2. Teschner D, Vass E, Hävecker M, Zafeiratos S, Schnörch P, Sauer H, Knop-Gericke A, Schlögl R, Chamam M, Wootsch A, Canning AS, Gamman JJ, Jackson SD, McGregor J, Gladden LF (2006) Alkyne hydrogenation over Pd catalysts: A new paradigm. J Catal 242 (1):26–37
3. Niemantsverdriet JW (1995) Spectroscopy in Catalysis. Wiley-VCH, Weinheim
4. Che M, Vedrine JC (eds) (2012) Characterization of Solid Materials and Heterogeneous Catalysts - From Structure to Surface Reactivity. Wiley-VCH, Weinheim
5. Weckhuysen BM, van der Voort P, Catana G (eds) (2000) Spectroscopy of Transition Metal Ions on Surfaces. Leuven University Press, Leuven
6. Haw JF (ed) (2002) In-situ Spectroscopy in Heterogeneous Catalysis. Wiley-VCH, Weinheim
7. Weckhuysen BM (ed) (2004) In-Situ Spectroscopy of Catalysts. Amer Scientific Pub, California
8. Hansen PL, Wagner JB, Helveg S, Rostrup-Nielsen JR, Clausen BS, Topsøe H (2002) Atom-resolved imaging of dynamic shape changes in supported copper nanocrystals. Science 295 (5562):2053–2055
9. Clausen BS, Schiøtz J, Gråbæk L, Ovesen CV, Jacobsen KW, Nørskow JK, Topsøe H (1994) Wetting/non-wetting phenomena during catalysis: Evidence from in situ on-line EXAFS studies of Cu-based catalysts. Top Catal 1 (3–4):367–376
10. Grunwaldt J-D, Molenbroek AM, Topsøe N-Y, Topsøe H, Clausen BS (2000) In Situ investigations of structural changes in Cu/ZnO catalysts. J Catal 194 (2):452–460
11. Wagner JB, Timpe O, Hamid FA, Trunschke A, Wild U, Su DS, Widi RK, Abd Hamid SB, Schlögl R (2006) Surface texturing of Mo–V–Te–Nb–Ox selective oxidation catalysts. Top Catal 38 (1–3):51–58
12. Sanfiz AC, Hansen TW, Teschner D, Schnörch P, Girgsdies F, Trunschke A, Schlögl R, Looi MH, Abd Hamid SB (2010) Dynamics of the MoVTeNb Oxide M1 Phase in Propane Oxidation. J Phys Chem C 114 (4):1912–1921
13. Millet JMM, Roussel H, Pigamo A, Dubois JL, Jumas JC (2002) Characterization of tellurium in MoVTeNbO catalysts for propane oxidation or ammoxidation. Appl Catal A 232 (1–2):77–92
14. Ueda W, Vitry D, Katou T (2004) Structural organization of catalytic functions in Mo-based oxides for propane selective oxidation. Catal Today 96 (4):235–240
15. Farges F, Brown GE, Rehr JJ (1997) Ti K-edge XANES studies of Ti coordination and disorder in oxide compounds: Comparison between theory and experiment. Phys Rev B 56 (4):1809–1819
16. Häggblad R, Hansen S, Wallenberg LR, Andersson A (2010) Stability and performance of cation vacant $Fe_{3-x-y}V_{xy}O_4$ spinel phase catalysts in methanol oxidation. J Catal 276 (1):24–37
17. Petit P-E, Farges F, Wilke M, Solé VA (2001) Determination of the iron oxidation state in Earth materials using XANES pre-edge information. J Synchrotron Rad 8:952–954
18. Farges F, Lefrère Y, Rossano S, Berthereau A, Calas G, Brown Jr GE (2004) The effect of redox state on the local structural environment of iron in silicate glasses: a combined XAFS spectroscopy, molecular dynamics, and bond valence study. J Non-Cryst Solids 344 (3):176–188
19. Reichinger M, Schmidt W, van den Berg MWE, Aerts A, Martens JA, Kirschhock CEA, Gies H, Grünert W (2009) Alkene epoxidation with mesoporous materials assembled from TS-1 seeds – Is there a hierarchical pore system? J Catal 269 (2):367–375
20. Glatzel JPS, Bergmann U (2005) High resolution 1 s core hole X-ray spectroscopy in 3d transition metal complexes - electronic and structural information. Coord Chem Rev 249 (1–2):65–95

21. Salmeron M, Schlögl R (2008) Ambient pressure photoelectron spectroscopy: A new tool for surface science and nanotechnology. Surf Sci Rep 63 (4):169–199
22. Ogletree DF, Bluhm H, Lebedev G, Fadley CS, Hussain Z, Salmeron M (2002) A differentially pumped electrostatic lens system for photoemission studies in the millibar range. Rev Sci Instr 73 (11):3872–3877
23. Bañares MA, Wachs IE (2002) Molecular structures of supported metal oxide catalysts under different environments. J Raman Spectrosc 33 (5):359–380
24. Zecchina A, Garrone E, Ghiotti G, Morterra C, Borello E. (1975) Chemistry of silica supported chromium ions. I. Characterization of the samples. J Phys Chem 79 (10):966–972
25. Topsøe N-Y, Topsøe H (1983) Characterization of the structures and active sites in sulfided Co-Mo/Al_2O_3 and Ni-Mo/Al_2O_3 catalysts by NO chemisorption. J Catal 84 (2):386–401
26. Zaki MI, Vielhaber B, Knözinger H (1986) Low-temperature carbon monoxide adsorption and state of molybdena supported on alumina, titania, ceria, and zirconia. An infrared spectroscopic investigation. J Phys Chem 90 (14):3176–3183
27. Hadjiivanov KI, Vayssilov GN (2002) Characterization of oxide surfaces and zeolites by carbon monoxide as an IR probe molecule. Adv Catal 47:307–511
28. Topsøe N-Y, Topsøe H (1999) FTIR studies of dynamic surface structural changes in Cu-based methanol synthesis catalysts. J Mol Catal A 141 (1–3):95–105
29. Elmasides C, Kondarides DI, Grünert W, Verykios XE (1999) XPS and FTIR Study of Ru/Al_2O_3 and Ru/TiO_2 Catalysts: Reduction Characteristics and Interaction with a Methane-Oxygen Mixture. J Phys Chem B 103 (25):5227–5239
30. Santhosh Kumar M, Schwidder M, Grünert W, Brückner A (2004) On the nature of different iron sites and their catalytic role in Fe-ZSM-5 DeNO_x catalysts: new insights by a combined EPR and UV/VIS spectroscopic approach. J Catal 227 (2):384–397
31. Brückner A (2004) Electron Paramagnetic Resonance. In: Weckhuysen BM (ed) (2004) In-situ Spectroscopy of Catalysts. Amer Scientific Pub, California
32. Blasco T. (2010) Insights into reaction mechanisms in heterogeneous catalysis revealed by in situ NMR spectroscopy. Chem. Soc. Rev. 39: 4685–4702
33. Steinfeldt N, Müller D, Berndt H (2004) VO_x species on alumina at high vanadia loadings and calcination temperature and their role in the ODP reaction. Appl Catal A 272 (1–2):201–213
34. Holland GP, Cherry BR, Alam TM (2004) N-15 solid-state NMR characterization of ammonia adsorption environments in 3A zeolite molecular sieves. J. Phys. Chem. B 108:16420–16426
35. Hunger M (2008) In situ flow MAS NMR spectroscopy: State of the art and applications in heterogeneous catalysis. Prog Nucl Magn Reson Spectrosc 53 (3):105–127
36. Chen H-Y, Sachtler WMH (1998) Activity and durability of Fe/ZSM-5 catalysts for lean-burn NO_x reduction in the presence of water vapor. Catal Today 42 (1–2):73–83
37. Heinrich F, Schmidt C, Löffler E, Menzel M, Grünert W (2002) Fe-ZSM-5 catalysts for the selective reduction of NO by isobutane - The problem of the active sites. J Catal 212 (2):157–172
38. Heinrich F (2002) Selektive katalytische Reduktion von NO mit Kohlenwasserstoffen an eisenmodifizierten Zeolithen. PhD thesis, Ruhr University, Bochum
39. Wilmer H, Genger T, Hinrichsen O (2003) The interaction of hydrogen with alumina-supported copper catalysts: a temperature-programmed adsorption/temperature-programmed desorption/isotopic exchange reaction study. J Catal 215 (2):188–198
40. Bond GC, Tahir SF (1991) Vanadium oxide monolayer catalysts - Preparation, characterization and catalytic activity. Appl Catal 71 (1):1–31
41. Centi G (1996) Nature of active layer in vanadium oxide supported on titanium oxide and control of its reactivity in the selective oxidation and ammoxidation of alkylaromatics. Appl Catal A 147 (2):267–298
42. Wachs IE (2005) Recent conceptual advances in the catalysis science of mixed metal oxide catalytic materials. Catal Today 100 (1–2):79–94

43. Wachs IE (1996) Raman and IR studies of surface metal oxide species on oxide supports: Supported metal oxide catalysts. Catal Today 27 (3–4):437–455
44. Deo G, Wachs IE, Haber J (1994) Supported vanadium-oxide catalysts - molecular structural characterization and reactivity properties. Crit Rev Surf Chem 4 (3–4):141–187
45. Eberhardt MA, Houalla M, Hercules DM (1993) Ion scattering and electron spectroscopic study of the surface coverage of V/Al_2O_3 catalysts. Surf Interface Anal 20 (9):766–770
46. Vaidyanathan N, Houalla M, Hercules DM (1997) Determination of the surface coverage of WO_3/TiO_2 catalysts by CO_2 chemisorption. Catal Lett 43 (3–4):209–212
47. Zingg DS, Makovsky LE, Tischer RE, Brown FR, Hercules DM (1980) A surface spectroscopic study of molybdenum-alumina catalysts using x-ray photoelectron, ion scattering, and Raman spectroscopies. J Phys Chem 84 (22):2898–2906
48. Briand LE, Tkachenko OP, Guraya M, Gao X, Wachs IE, Grünert W (2004) Surface-analytical Studies of Supported Vanadium Oxide Monolayer Catalysts. J Phys Chem B 108 (15):4823–4830
49. Briand LE, Tkachenko OP, Guraya M, Wachs IE, Grünert W (2004) Methodical aspects in the surface analysis of supported molybdena catalysts. Surf Interface Anal 36 (3):238–245
50. Leyrer J, Zaki MI, Knözinger H (1990) Solid/solid interactions - Monolayer formation in MoO_3/Al_2O_3 physical mixtures. J Phys Chem 90 (20):4775–4780
51. Xie Y, Gui L, Liu Y, Zhao B, Yang N, Zhang Y, Guo Q, Duan L, Huang H, Cai X, Tang Y (1984) In: Proceedings of the 8th International Congress on Catalysis. Berlin, 5:147
52. Kompio PGWA, Brückner A, Hipler F, Auer G, Löffler E, Grünert W (2012) A new view on the relations between tungsten and vanadium in V_2O_5-WO_3/TiO_2 catalysts for the selective reduction of NO with NH_3. J Catal 286:237–247
53. Inomata M, Miyamoto A, Murakami Y (1980) Mechanism of the reaction of NO and NH_3 on vanadium oxide catalyst in the presence of oxygen under the dilute gas condition. J Catal 62 (1):140–148
54. Baiker A, Dollenmeier P, Glinski M, Reller A (1987) Selective catalytic reduction of nitric oxide with ammonia: I. Monolayer and Mulitlayers of Vanadia Supported on Titania. Appl Catal 35 (2):351–364
55. Went GT, Leu LJ, Rosin RR, Bell AT (1992) The effects of structure on the catalytic activity and selectivity of V_2O_5/TiO_2 for the reduction of NO by NH_3. J Catal 134 (2):492–505
56. Lietti L, Forzatti P (1994) Temperature Programmed Desorption/Reaction of Ammonia over V_2O_5/TiO_2 De-NO_xing Catalysts. J Catal 147 (1):241–249
57. Szakacs S, Altena GJ, Fransen T, Van Ommen JG, Ross JRH (1993) The Selective Reduction of NO_x with NH_3 over Zirconia-Supported Vanadia Catalysts. Catal Today 16 (2):237–245
58. Bosch H, Janssen FJJG (1988) Catal Today 2 (4):369–531
59. Ozkan US, Cai YP, Kumthekar MW (1994) Investigation of the Reaction Pathways in Selective Catalytic Reduction of NO with NH_3 over V_2O_5 Catalysts: Isotopic Labeling Studies Using $^{18}O_2$, $^{15}NH_3$, ^{15}NO, and $^{15}N^{18}O$. J Catal 149 (2):390–403
60. Gasior M, Haber J, Machej T, Czeppe T (1988) Mechanism of the reaction NO + NH_3 on V_2O_5 catalysts. J Mol Catal 43 (3):359–369
61. Topsøe N-Y (1994) Mechanism of the Selective Catalytic Reduction of Nitric Oxide by Ammonia Elucidated by in Situ On-Line Fourier Transform Infrared Spectroscopy. Science 265 (5176):1217–1219
62. Topsøe N-Y, Dumesic JA, Topsøe H (1995) Vanadia-Titania Catalysts for Selective Catalytic Reduction of Nitric-Oxide by Ammonia .2. Studies of Active-Sites and Formulation of Catalytic Cycles. J Catal 151 (1):241–252
63. Topsøe N-Y, Topsøe H, Dumesic JA (1995) Vanadia-Titania Catalysts for Selective Catalytic Reduction (SCR) of Nitric-Oxide by Ammonia .1. Combined Temperature-Programmed in-Situ FTIR and Online Mass-Spectroscopy Studies. J Catal 151 (1):226–240

64. Dumesic JA, Topsøe N-Y, Topsøe H, Chen Y, Slabiak T (1996) Kinetics of Selective Catalytic Reduction of Nitric Oxide by Ammonia over Vanadia/Titania. J Catal 163 (2):409–417
65. Wark M, Brückner A, Liese T, Grünert W (1998) Selective Catalytic Reduction of NO by NH_3 over Vanadium- Containing Zeolites. J Catal 175(1):48–61
66. Alemany LJ, Lietti L, Ferlazzo N, Forzatti P, Busca G, Giamello E, Bregani F (1995) Reactivity and Physicochemical Characterization of V_2O_5-WO_3/TiO_2 De-NO_x Catalysts. J Catal 155 (1):117–130
67. Broclawik E, Góra A, Najbar M (2001) The role of tungsten in formation of active sites for no SCR on the V-W-O catalyst surface - quantum chemical modeling (DFT). J Mol Catal A 166 (1):31–38
68. Lietti L, Alemany JL, Forzatti P, Busca G, Ramis G, Giamello E, Bregani F (1996) Reactivity of V_2O_5-WO_3/TiO_2 catalysts in the selective catalytic reduction of nitric oxide by ammonia. Catal Today 29 (1–4):143–148
69. Vuurman MA, Wachs IE, Hirt AM (1991) Structural determination of supported vanadium pentoxide-tungsten trioxide-titania catalysts by in situ Raman spectroscopy and x-ray photoelectron spectroscopy. J Phys Chem 95 (24):9928–9937
70. Kompio PGWA (2010) Der Einfluss von Hochtemperaturbehandlungen auf V_2O_5-WO_3/TiO_2-Katalysatoren für die selektive katalytische Reduktion von Stickoxiden mit Ammoniak. PhD thesis, Ruhr University; Bochum
71. Feng X, Hall WK (1996) On the unusual stability of overexchanged FeZSM-5. Catal Lett 41 (1–2):45–46
72. Voskoboinikov TV, Chen H-Y, Sachtler WMH (1998) On the nature of active sites in Fe/ZSM-5 catalysts for NO_x abatement. Appl Catal B 19 (3–4):279–287
73. Chen H-Y, El-Malki E-M, Wang X, Van Santen RA, Sachtler WMH (2000) Identification of active sites and adsorption complexes in Fe/MFI catalysts for NO_x reduction. J Mol Catal A 162 (1–2):159–174
74. Iwamoto M, Yahiro H, Tanda K, Mizuno N, Mine Y, Kagawa S (1991) Removal of Nitrogen Monoxide through a Novel Catalytic Process. 1. Decomposition on Excessively Copper Ion Exchanged ZSM-5 Zeolites. J Phys Chem 95 (9):3727–3730
75. Battiston AA, Bitter JH, Koningsberger DC (2000) XAFS characterization of the binuclear iron complex in overexchanged Fe/ZSM5 - structure and reactivity. Catal Lett 66 (1–2):75–79
76. Marturano P, Drozdová L, Kogelbauer A, Prins R (2000) Fe/ZSM-5 Prepared by Sublimation of $FeCl_3$: The Structure of the Fe Species as Determined by IR, ^{27}Al MAS NMR, and EXAFS Spectroscopy. J Catal 192 (1):236–247
77. Marturano P, Drozdová L, Pirngruber GD, Kogelbauer A, Prins R (2001) The mechanism of formation of the Fe species in Fe/ZSM-5 prepared by CVD. PCCP 3:5585–5595
78. Battiston AA, Bitter JH, Koningsberger DC (2003) Reactivity of binuclear Fe complexes in over-exchanged Fe/ZSM5, studied by in situ XAFS spectroscopy – 2. Selective catalytic reduction of NO with isobutane. J Catal 218 (1):163–177
79. Heinrich F, Schmidt C, Löffler E, Grünert W (2001) A highly active intra-zeolite iron site for the selective catalytic reduction of NO by isobutane. Catal Comm 2 (10):317–321
80. Heijboer WM, Koningsberger DC, Weckhuysen BM, de Groot FMF (2005) New frontiers in X-ray spectroscopy in heterogeneous catalysis: Using Fe/ZSM-5 as test-system. Catal Today 110 (3–4):228–238
81. Battiston AA, Bitter JH, de Groot FMF, Overweg AR, Stephan O, van Bokhoven JA, Kooyman PJ, van der Spek C, Vankó G, Koningsberger DC (2003) Evolution of Fe species during the synthesis of over-exchanged Fe/ZSM5 obtained by chemical vapor deposition of $FeCl_3$. J Catal 213 (2):251–271
82. Pirngruber GD, Roy PK, Prins R (2006) On determining the nuclearity of iron sites in Fe-ZSM-5 - a critical evaluation. Phys Chem Chem Phys 8 (34):3939–3950
83. Long RQ, Yang RT (2001) Fe-ZSM-5 for selective catalytic reduction of NO with NH_3: a comparative study of different preparation techniques. Catal Lett 74 (3–4):201–205

84. Berrier E, Ovsitser O, Kondratenko EV, Schwidder M, Grünert W, Brückner A (2007) Temperature-dependent N_2O decomposition over Fe-ZSM-5: Identification of sites with different activity. J Catal 249 (1):67–78
85. Bordiga S, Buzzoni R, Geobaldo F, Lamberti C, Giamello E, Zecchina A, Leofanti G, Petrini G, Tozzola G, Vlaic G (1996) Structure and reactivity of framework and extraframework iron in Fe-silicate as investigated by spectroscopic and physicochemical methods. J Catal 158 (2):486–501
86. Schwidder M, Santhosh Kumar M, Klementiev KV, Pohl MM, Brückner A, Grünert W (2005) Selective Reduction of NO with Fe-ZSM-5 Catalysts of Low Fe content I. Relations between Active Site Structure and Catalytic Performance. J Catal 231 (2):314–330
87. Santhosh Kumar M, Schwidder M, Grünert W, Bentrup U, Brückner A (2006) Selective reduction of NO with Fe-ZSM-5 catalysts of low Fe content. II. Assigning the function of different Fe sites by spectroscopic in situ studies. J Catal 239 (1):173–186
88. Schwidder M, Heikens S, De Toni A, Geisler S, Berndt M, Brückner A, Grünert W (2008) The role of NO_2 in the Selective Catalytic Reduction of Nitrogen Oxides over Fe-ZSM-5 Catalysts – Active Sites for the Conversion of NO and of NO/NO_2 mixtures. J Catal 259 (1):96–103
89. Krishna K, Makkee M (2006) Preparation of Fe-ZSM-5 with enhanced activity and stability for SCR of NO_x. Catal Today 114 (1):23–30
90. Doronkin DE, Stakheev AY, Kucherov AV, Tolkachev NN, Kustova M, Høj M, Baeva GN, Bragina GO, Gabrielsson P. Gekas I, Dahl S (2009) Nature of Active Sites of Fe-Beta Catalyst for NO_x-SCR by NH_3. Top Catal 52 (13–20):1728–1733
91. Klukowski D, Balle P, Geiger B, Waglöhner S, Kureti S, Kimmerle B, Baiker A, Grunwaldt J-D (2009) On the mechanism of the SCR reaction on Fe/HBEA zeolite. Appl Catal B 93 (1–2):185–193
92. Iwasaki M, Yamazaki K, Banno K, Shinjoh H (2008) Characterization of Fe/ZSM-5 DeNO_x catalysts prepared by different methods: Relationships between active Fe sites and NH_3-SCR performance. J Catal 260 (2):205–216
93. Iwasaki M, Shinjoh H (2010) Analysis of the adsorption state and desorption kinetics of NO_2 over Fe-zeolite catalysts by FTIR and temperature programmed desorption. Phys Chem Chem Phys 12 (10):2365–2372
94. Iwasaki M, Shinjoh H (2010) NO evolution reaction with NO_2 adsorption over Fe/ZSM-5: In situ FT-IR observation and relationships with Fe sites. J Catal 273 (1):29–38
95. Dědeček J, Sobalik Z, Wichterlová B (2012) Siting and Distribution of Framework Aluminium Atoms in Silicon-Rich Zeolites and Impact on Catalysis. Catal Rev Sci Eng 54:135–223
96. Sobalik Z, Sazama P, Dědeček J, Wichterlová B Critical evaluation of the role of the distribution of Al atoms in the framework for the activity of metallo-zeolites in redox N_2O/NO_x reactions Appl Catal A 2014: in press doi: 10.1016/j.apcata.2013.07.033
97. Brandenberger S, Kröcher O, Tissler A, Althoff R (2008) The state of the art in selective catalytic reduction of NO_x by ammonia using metal-exchanged zeolite catalysts. Catal Rev - Sci Eng 50 (4):492–531
98. Brandenberger S, Kröcher O (2010) Estimation of the fractions of different nuclear iron species in uniformly metal-exchanged Fe-ZSM-5 samples based on a Poisson distribution. Appl Catal B 373 (1–2):168–175
99. Brandenberger S, Kröcher O, Tissler A, Althoff R (2010) The determination of the activities of different iron species in Fe-ZSM-5 for SCR of NO by NH_3. Appl Catal B 95 (3–4):348–357
100. Schwidder M, Santhosh Kumar M, Bentrup U, Pérez-Ramírez J, Brückner A, Grünert W (2008) The role of Brønsted Acidity in the SCR of NO over Fe-MFI Catalysts. Microporous Mesopor Mater 111 (1–3):124–133
101. Brandenberger S, Kröcher O, Wokaun A, Tissler A, Althoff R (2010) The role of Brønsted acidity in the selective catalytic reduction of NO with ammonia over Fe-ZSM-5. J Catal 268 (2):297–306

102. Yeom YH, Henao J, Li MJ, Sachtler WMH, Weitz E (2005) The role of NO in the mechanism of NO_x reduction with ammonia over a BaNa-Y catalyst. J Catal 231 (1):181–193
103. Li MJ, Yeom Y, Weitz E, Sachtler WMH (2006) An acid catalyzed step in the catalytic reduction of NO_x to N_2. Catal Lett 112 (3–4):129–132
104. Pérez Vélez R, Ellmers I, Huang H, et al. Identifying active sites for fast NH3-SCR of NO/NO_2 mixtures over Fe-ZSM-5 by operando EPR and UV-vis spectroscopy. J Catal 2014:submitted
105. Ellmers I, Velez RP, Bentrup U, Brückner A, Grünert W (2014) Oxidation and Selective Reduction of NO over Fe-ZSM-5 – How related are these reactions? J. Catal 311:199–211 in press.
106. Apostolescu N, Geiger B, Hizbullah K, Jan MT, Kureti S, Reicher D, Schott F, Weisweiler W (2006) Selective catalytic reduction of nitrogen oxides by ammonia on iron oxide catalysts. Appl Catal B 62 (1–2):104–114
107. Centi G, Perathoner S (1995) Nature of active species in copper-based catalysts and their chemistry of transformation of nitrogen oxides. Appl Catal A 132 (2):179–259
108. Seiyama T, Arakawa T, Matsuda T, Yamazoe N, Takita Y (1975) Catalytic Reduction of Nitric-oxide with Ammonia over Transition-metal Ion-exchanged Y-zeolites. Chem Lett 4 (7):781–784
109. Seiyama T, Arakawa T, Matsuda T, Takita Y, Yamazoe N (1977) Catalytic activity of transition metal ion exchanged Y zeolites in the reduction of nitric oxide with ammonia. J Catal 48 (1–3):1–7
110. Iwamoto M, Yahiro H, Mine Y, Kagawa S (1989) Excessively Copper ion-exchanged ZSM-5 zeolites as highly active catalyst for direct decomposition of nitrogen monoxide. Chem Lett 18 (2):213
111. Held W, König A, Richter T, Puppe L (1990) Catalytic NO_x reduction in net oxidizing exhaust gas. SAE-Technical Paper: 900496 doi: 10.4271/900496
112. Williamson WB, Lunsford JH (1976) Nitric oxide reduction with ammonia over copper(II) Y zeolites. J Phys Chem 80 (24):2664–2671
113. Campa MC, Indovina V, Minelli G, Moretti G, Pettiti I, Porta A, Riccio A (1994) The catalytic activity of Cu-ZSM-5 and Cu-Y zeolites in NO decomposition: dependence on copper concentration. Catal Lett 23 (1–2):141–149
114. Valyon J, Keith Hall W (1993) On the preparation and properties of Cu-ZSM-5 catalysts for NO decomposition. Catal Lett 19 (2–3):109–119
115. Moretti G (1994) Turnover frequency for NO decomposition over Cu-ZSM-5 catalysts: insight into the reaction mechanism. Catal Lett 28 (2–4):143–152
116. Lei GD, Adelman BJ, Sárkáni J, Sachtler WMH (1995) Identification of copper(II) and copper(I) and their interconversion in Cu/ZSM-5 De-NO_x catalysts. Appl Catal B 5 (3):245–256
117. Moretti G, Ferraris G, Fierro G, Lo Jacono M, Morpurgo S, Faticanti M (2005) Dimeric Cu(I) species in Cu-ZSM-5 catalysts: the active sites for the NO decomposition. J Catal 232 (2):476–487
118. Sárkány J, d'Itri JL, Sachtler WMH (1992) Redox chemistry in excessively ion-exchanged Cu/Na-ZSM-5. Catal Lett 16 (3):241–249
119. Wichterlová B, Dedecek J, Tvaružková Z (1994) Cu coordination in zeolite matrix. Relationship to nitric oxide binding and decomposition. Stud Surf Sci Catal 84 :1555–1562
120. Grünert W, Hayes NW, Joyner RW, Shpiro ES, Siddiqui MRH, Baeva GN (1994) Structure, Chemistry, and Activity of Cu-ZSM-5 Catalysts for the Selective Reduction of NO_x in the Presence of Oxygen. J Phys Chem 98 (42):10832–10846
121. Liese T, Grünert W (1997) Cu-Na-ZSM-5 Catalysts Prepared by Chemical Transport: Investigations on the Role of Brønsted Acidity and of Excess Copper in the Selective Catalytic Reduction of NO by Propene. J Catal 172 (1):34–45
122. Jirka I, Wichterlová B, Maryská M (1991) ESCA study of incorporation of copper into Y zeolite. Stud Surf Sci Catal 69 (1):269–276

123. Sexton BA, Smith TD, Sanders JV (1985) Characterization of copper-exchanged Na-A, X and Y zeolites with X-ray photoelectron spectroscopy and transmission electron microscopy. J Electron Spectrosc Relat Phenom 35 (1):27–43
124. Morales J, Espinos JP, Caballero A, Gonzalez-Elipe AR, Mejias JA (2005) XPS study of interface and ligand effects in supported Cu_2O and CuO nanometric particles. J Phys Chem B 109 (16):7758–7765
125. Sato S, Yu-u Y, Yahiro H, Mizuno N, Iwamoto M (1991) Cu-ZSM-5 zeolite as highly active catalyst for removal of nitrogen monoxide from emission of diesel engines. Appl Catal 70 (1):L1–L5
126. Kharas KCC (1993) Performance, selectivity, and mechanism in Cu-ZSM-5 lean-burn catalysts. Appl Catal B 2 (2–3):207–224
127. Ciambelli P, Corbo P, Gambino M, Minelli G, Moretti G, Porta P (1995) Lean NOx reduction CuZSM5 catalysts: Evaluation of performance at the spark ignition engine exhaust. Catal Today 26 (1):33–39
128. Wichterlová B, Sobalik Z, Vondrová A (1996) Differences in the structure of copper active sites for decomposition and selective reduction of nitric oxide with hydrocarbons and ammonia. Catal Today 29 (1–4):149–153
129. Centi G, Nigro C, Perathoner S, Stella G (1994) Reactivity of Cu-Based Zeolites and Oxides in the Conversion of NO in the Presence or Absence of O_2. Environmental Catalysis: ACS Symposium Ser. 552 (3):22–38
130. Shelef M (1995) Selective catalytic reduction of NO_x with N-free reductants. Chem Rev 95 (1):209–225
131. Hamada H, Kintaichi Y, Sasaki M, Ito T, Tabata M (1990) Highly selective reduction of nitrogen oxides with hydrocarbons over H-form zeolite catalysts in oxygen-rich atmosphere. Appl Catal 64 (1–2):L1–L4
132. Loughran CE, Resasco DE (1995) Bifunctionality of palladium-based catalysts in the reduction of nitric oxide by methane in the presence of oxygen. Appl Catal B 7 (1–2):113–126
133. Kikuchi E, Yogo K (1994) Selective catalytic reduction of nitrogen monoxide by methane on zeolite catalysts in an oxygen-rich atmosphere. Catal Today 22 (1):73–86
134. Centi G, Perathoner S, Dall'Olio L (1994) High activity of copper-boralite in the reduction of nitric oxide with propane/oxygen. Appl Catal B 4 (4):L275–L281
135. Jen H-W, McCabe RW, Gorte RJ, Parillo DJ (1994) Reduction of NO Under Lean Conditions Over ZSM-5-Based Catalysts: Effect of Cu Loading and Zeolite Type. Am Chem Soc, Div Petr Chem 39:104–109
136. Kieger S, Delahay G, Coq B, Neveu B (1999) Selective Catalytic Reduction of Nitric Oxide by Ammonia over Cu-FAU Catalysts in Oxygen-Rich Atmosphere. J Catal 183 (2):267–280
137. Komatsu T, Nunokawa M, Moon IS, Takahara T, Namba S, Yashima T (1994) Kinetic Studies of Reduction of Nitric Oxide with Ammonia on Cu^{2+}-Exchanged Zeolites. J Catal 148 (2):427–437
138. Fickel DW, Lobo RF (2010) Copper Coordination in Cu-SSZ-13 and Cu-SSZ-16 Investigated by Variable-Temperature XRD. J Phys Chem C 114 (3):1633–1640
139. Korhonen ST, Fickel DW, Lobo RF, Weckhuysen BM, Beale AM (2011) Isolated Cu^{2+} ions: active sites for selective catalytic reduction of NO. Chem Commun 47 (47):800–802
140. Fickel DW, D'Addio E, Lauterbach JA, Lobo RF (2011) The ammonia selective catalytic reduction activity of copper-exchanged small-pore zeolites. Appl Catal B 102 (3–4):441–448
141. Deka U, Juhin A, Eilertsen EA, Emerich H, Green MA, Korhonen ST, Weckhuysen BM, Beale AM (2012) Confirmation of Isolated Cu2 + Ions in SSZ-13 Zeolite as Active Sites in NH_3-Selective Catalytic Reduction. J Phys Chem C 116 (7):4809–4818
142. Kwak JH, Zhu H, Lee JH, Peden CHF, Szanyi J (2012) Two different cationic positions in Cu-SSZ-13? Chem Commun 48 (39):4758–4760
143. Kwak JH, Tran D, Burton SD, Szanyi J, Jolee JH, Peden CHF (2012) Effects of hydrothermal aging on NH_3-SCR reaction over Cu/zeolites. J Catal 287 (1):203–209

144. Li J, Chang H, Ma L, Hao J, Yang RT (2011) Low-temperature selective catalytic reduction of NO_x with NH_3 over metal oxide and zeolite catalysts-A review. Catal Today 175 (1):147–156
145. Kapteijn F, Singoredjo L, Andreini A, Moulijn JA (1994) Activity and selectivity of pure manganese oxides in the selective catalytic reduction of nitric oxide with ammonia. Appl Catal B 3 (2–3):173–189
146. Tang X, Li J, Sun L, Hao J (2010) Origination of N_2O from NO reduction by NH_3 over Beta-MnO_2 and alpha-Mn_2O_3. Appl Catal B 99 (1–2):156–162
147. Yoshikawa M, Yasutake A, Mochida I (1998) Low-Temperature selective catalytic reduction of NOx by metal oxides supported on active carbon fibers. Appl Catal A173 (2):239–245
148. Grzybek T, Klinik J, Rogoz M, Papp H (1998) Manganese supported catalysts for selective catalytic reduction of nitrogen oxides with ammonia - Part 1 - Characterization. J Chem Soc-Faraday Trans 94 (18):2843–2850
149. Grzybek T, Pasel J, Papp H (1999) Supported manganese catalysts for the selective catalytic reduction of nitrogen oxides with ammonia II. Catalytic experiments. Phys Chem Chem Phys 1 (2):341–348
150. Qi G, Yang RT (2003) Low-temperature selective catalytic reduction of NO with NH_3 over iron and manganese oxides supported on titania. Appl Catal B 44 (3):217–225
151. Ettireddy PR, Ettireddy N, Mamedov S, Boolchand P, Smirniotis PG (2007) Surface characterization studies of TiO_2 supported manganese oxide catalysts for low temperature SCR of NO with NH_3. Appl Catal B 76 (1–2):123–134
152. Pena DA, Uphade BS, Smirniotis PG (2004) TiO_2-supported metal oxide catalysts for low-temperature selective catalytic reduction of NO with NH_3: I. Evaluation and characterization of first row transition metals. J Catal 221 (2):421–431
153. Zhuang K, Qiu J, Tang F, Xu B, Fan Y (2011) The structure and catalytic activity of anatase and rutile titania supported manganese oxide catalysts for selective catalytic reduction of NO by NH_3. Phys Chem Chem Phys 13 (10):4463–4469
154. Marbán G, Valdés-Solís T, Fuertes A (2004) Mechanism of low-temperature SCR of NO with NH_3 over carbon-supported Mn_3O_4. Phys Chem Chem Phys 6 (2):453–464
155. Marbán G, Valdés-Solís T, Fuertes AB (2004) Mechanism of low-temperature selective catalytic reduction of NO with NH_3 over carbon-supported Mn_3O_4: Role of surface NH_3 species: SCR mechanism. J Catal 226 (1):138–155
156. Kapteijn F, Singoredjo L, Vandriel M, Andreini A, Moulijn JA, Ramis G, Busca G (1994) Alumina-Supported Manganese Oxide Catalysts .2. Surface Characterization and Adsorption of Ammonia and Nitric-Oxide. J Catal 150 (1):105–116
157. Kijlstra WS, Brands DS, Poels EK, Bliek A (1997) Mechanism of the Selective Catalytic Reduction of NO by NH_3 over MnO_x/Al_2O_3. J Catal 171 (1):208–218
158. Kijlstra WS, Brands DS, Smit HI, Poels EK, Bliek A (1997) Mechanism of the Selective Catalytic Reduction of NO with NH_3 over MnO_x/Al_2O_3. J Catal 171 (1):219–230
159. Li J, Chen J, Ke R, Luo C, Hao J. Effects of precursors on the surface Mn species and the activities for NO reduction over MnO_x/TiO_2 catalysts (2007) Catal Commun 8 (12):1896–1900
160. Biesinger MC, Payne BP, Grosvenor AP, Lau LW M, Gerson AR, Smart RSC (2011) Resolving surface chemical states in XPS analysis of first row transition metals, oxides and hydroxides: Cr, Mn, Fe, Co and Ni. Appl Surf Sci 257 (7):2717–2730
161. Murray JW, Dillard JG, Giovanoli R, Moers H, Stumm W (1985) Oxidation of Mn(II): Initial mineralogy, oxidation state and ageing. Geochimica et Cosmochimica Acta 49 (2):463–470
162. Long RQ, Yang RT, Chang R (2002) Low temperature selective catalytic reduction (SCR) of NO with NH_3 over Fe-Mn based catalysts. Chem Comm (5):452–453
163. Chen Z, Yang Q, Li H, Li X, Wang L, Tsang SC (2010) Cr-MnO_x mixed-oxide catalysts for selective catalytic reduction of NO_x with NH_3 at low temperature. J Catal 276 (1):56–65

164. Chen ZH, Wang FR, Li H, Wang L, Yang Q, Li X (2011) Low-Temperature Selective Catalytic Reduction of NO_x with NH_3 over Fe-Mn Mixed-Oxide Catalysts Containing $Fe_3Mn_3O_8$ Phase. Ind Eng Chem Research 51 (1):202–212
165. Qi G, Yang RT, Chang R (2004) MnO_x-CeO2 mixed oxides prepared by co-precipitation for selective catalytic reduction of NO with NH_3 at low temperatures. Appl Catal B: Environ 51 (2):93–106
166. Shan W, Liu F, He H, Shi X, Zhang C (2011) The Remarkable Improvement of a Ce-Ti based Catalyst for NOx Abatement, Prepared by a Homogeneous Precipitation Method. Chem Cat Chem 3: (8)1286–1289
167. Li P, Xin Y, Li Q, Wang Z, Zhang Z, Zheng L (2012) Ce-Ti Amorphous Oxides for Selective Catalytic Reduction of NO with NH_3: Confirmation of Ce-O-Ti Active Sites. Environ Sci Tech 46 (17):9600–9605
168. Chen L, Li J, Ablikim W, Wang J, Chang H, Ma L, Xu J, Ge M, Arandiyan H (2011) CeO_2-WO_3 Mixed Oxides for the Selective Catalytic Reduction of NO_x by NH_3 Over a Wide Temperature Range. Catal Lett 141 (12):1859–1864
169. Chen L, Li J, Ge M (2010) DRIFT Study on Cerium-Tungsten/Titiania Catalyst for Selective Catalytic Reduction of NO_x with NH_3. Environ Sci Tech 44 (24):9590–9596